environments

MDPI

Article

Spatial Coherence and Non-Stationary Drought Dynamics in Water Management Basins of Northern and Central Kazakhstan

Makpal Dautaliyeva [1,2], Lyazzat Makhmudova [1], Elmira Talipova [1,2], Lyazzat Birimbayeva [1], Galymzhan Kambarbekov [2,3], Harris Vangelis [4], Aidana Daiyrbayeva [2], Madina Zhulkainarova [5], Adilet Kanatuly [5,*], María-Elena Rodrigo-Clavero [6] and Javier Rodrigo-Ilarri [6,*]

1 JSC "Institute of Geography and Water Security", Almaty 050000, Kazakhstan; masimbaeva@mail.ru (M.D.); mlk2002@mail.ru (L.M.); elmira_280386@mail.ru (E.T.); birimbayeva_l@mail.ru (L.B.)
2 Al-Farabi Kazakh National University, Almaty 050040, Kazakhstan; galakgm@gmail.com (G.K.); daiyrbayevaa@gmail.com (A.D.)
3 Water Resources Use Regulation Department of the Committee for Regulation, Protection and Use of Water Resources of the Ministry of Water Resources and Irrigation of the Republic of Kazakhstan, Astana 010000, Kazakhstan
4 Centre for the Assessment of Natural Hazards and Proactive Planning & Laboratory of Reclamation Worksand Water Resources Management, School of Rural, Surveying and Geoinformatics Engineering, National Technical University of Athens, Athens 15780, Greece; harrivag@central.ntua.gr
5 Department of Water Resources and Melioration, Kazakh National Agrarian Research University, Almaty 050010, Kazakhstan; madina942001@gmail.com
6 Instituto de Ingeniería del Agua y del Medio Ambiente (IIAMA), Universitat Politècnica de València, 46022 Valencia, Spain; marodcla@upv.es
* Correspondence: adilet31_2008@mail.ru (A.K.); jrodrigo@upv.es (J.R.-I.)

Highlights

What are the main findings?

- Drought regimes show non-stationary behavior across the studied basins.
- Major drought episodes were spatially coherent, especially in the Esil basin.
- SDI-12 revealed more stable hydrological drought conditions over time compared to short-term meteorological indices.

What are the implications of the main findings?

- Historical drought statistics should account for non-stationarity.
- Integrated SPI, SPEI, and SDI monitoring improves drought assessment.
- Results support basin-specific early warning and adaptive water management.

Abstract

This study investigates the spatiotemporal variability, spatial consistency, and non-stationarity of meteorological and hydrological droughts in three major water management basins (WMBs) of northern and central Kazakhstan: Nura–Sarysu, Esil, and Tobyl–Torgai. Long-term instrumental observations from meteorological stations and hydrological gauges were used to calculate the Standardized Precipitation Index (SPI), Standardized Precipitation Evapotranspiration Index (SPEI), and Streamflow Drought Index (SDI). Structural changes were detected using the Pettitt, Buishand, and CUSUM tests, while spatial consistency was quantitatively assessed as the proportion of active meteorological stations simultaneously experiencing drought conditions. The results showed that major drought episodes represented spatially coherent regional events rather than isolated local anomalies; however, their spatial extent varied substantially among the basins. The highest synchronization of meteorological droughts was observed in the Esil WMB, whereas the

Check for updates

Academic Editor: Guobin Fu

Received: 25 July 2026
Revised: 4 September 2026
Accepted: 14 September 2026
Published: 22 September 2026

Copyright: © 2026 by the authors. Licensee MDPI, Basel, Switzerland. This article is an open access article distributed under the terms and conditions of the Creative Commons Attribution (CC BY) license.

Tobyl–Torgai WMB exhibited greater spatial heterogeneity. Statistically significant structural changes were identified in both meteorological and hydrological drought series; however, their timing and frequency differed among indices and basins, indicating pronounced temporal non-stationarity. A higher proportion of structural changes was identified for SPI-3 than for SPEI-3. However, this difference is interpreted as reflecting differences in the statistical behavior of the precipitation index and the climatic water balance index rather than direct evidence of the relative contributions of precipitation and atmospheric evaporative demand. SDI-12 exhibited more persistent and temporally smoothed hydrological drought dynamics compared with the short-term meteorological indices, while the timing of hydrological changes differed among river systems. The results demonstrate that drought development in Northern and Central Kazakhstan is characterized by spatial heterogeneity and temporal non-stationarity, while the joint interpretation of SPI, SPEI, and SDI provides a more comprehensive basis for basin-scale drought monitoring and adaptive water-resource management.

Keywords: drought non-stationarity; spatial coherence; meteorological drought; hydrological drought; Kazakhstan water management basins

1. Introduction

Current climate change undoubtedly exerts, and will continue to exert, a significant influence on climate extremes, including drought events. Drought is a natural phenomenon characterized by a moisture deficit that occurs across various climatic zones and results in substantial damage. According to UN data, losses attributable to droughts exceed 20% of the total damage inflicted by all-natural disasters [1]. Droughts, particularly in their extreme forms, accelerate the process of desertification, which is primarily driven by excessive anthropogenic pressure exacerbated during prolonged and intense dry periods [2–6].

Droughts are among the most prevalent and severe natural hazards globally due to their frequency, broad spectrum of impacts, and protracted duration. They typically originate from water shortages resulting from the interaction of diverse factors, including meteorological conditions (precipitation deficits) and hydrological, hydrogeological, and water management factors [7–9].

Drought is a multifaceted phenomenon that can be analyzed from several perspectives. Most definitions of drought center on the concept of moisture deficit. Challenges in defining drought arise from the necessity of considering various components of the hydrological cycle, along with the specific timeframes and environments in which the moisture deficit manifests. The simultaneous occurrence of a prolonged moisture deficit in deep soil layers and a short-term moisture surplus in the topsoil reflects the inherent complexity involved in defining and identifying drought events.

According to the established classification [10,11], droughts can be categorized into meteorological, hydrological, agricultural, and socio-economic types, as they reflect water shortages resulting from an imbalance between water supply and demand across various sectors. Meteorological droughts, triggered by prolonged precipitation deficits, serve as the primary driver of other drought types. For instance, insufficient precipitation leads to reduced streamflow and inadequate groundwater recharge.

Any form of drought, whether meteorological, agricultural, or hydrological, exerts a substantial impact on water resources, agriculture, and food security. Consequently, understanding the mechanisms by which meteorological droughts propagate into agricultural and hydrological droughts is of critical importance for effective drought management.

Hydrological droughts manifest when streamflow and water storage in aquifers, lakes, and reservoirs fall below their long-term average values. Typically, a hydrological drought occurs with a specific time lag relative to a meteorological drought. Since regions are interconnected through hydrological systems, the spatial extent of a hydrological drought may exceed that of the meteorological drought that induced it. Correlating hydrological droughts with climatically driven precipitation deficits is frequently complicated by the simultaneous influence of non-climatic factors on basin characteristics, such as inefficient water resource management, land-use changes (including land degradation and soil erosion), and the construction of reservoirs and dams [12].

Hydrological droughts arise from various hydrometeorological processes (precipitation deficits, reduced snow cover, and high potential evapotranspiration), the magnitudes of which vary depending on the regional climate and the severity of the drought events. It is noted that the relative contribution of the various processes leading to drought may shift over the course of ongoing climate change. Such shifts can influence the intensity, duration, and magnitude of moisture deficits, as the various formative processes are linked to diverse environmental factors. For example, droughts triggered by precipitation deficits that persist in the dry season are associated with longer dry periods, in contrast to those resulting solely from a lack of precipitation. This observation underscores a critical concern: the transition toward more arid conditions due to climate warming that may exacerbate drought severity. Consequently, understanding the evolving processes behind hydrological drought formation is essential for projecting future changes [13].

Accordingly, the intensification of droughts driven by climate change and anthropogenic factors increases pressure on the hydrological cycle in water-stressed countries. Drought monitoring, specifically determining its onset, termination, and typology, is of paramount importance for water resource planning and management [12,14–16], particularly in Central Asia [12,17,18], one of the world's most arid regions. Increasing drought intensity and frequency are key factors impacting sustainable economic development and environmental security.

Despite a substantial body of research dedicated to the assessment of individual drought types, the spatial coherence of their occurrence, particularly under hydroclimatic non-stationarity at the scale of major river basins, remains insufficiently studied. Most published studies focus either on the analysis of isolated drought indices or on individual river basins, whereas a comprehensive assessment of the relationship between meteorological and hydrological droughts, their spatial coherence, and long-term variability remains limited.

This study attempts to address this gap through a comprehensive analysis of the spatiotemporal dynamics of meteorological and hydrological droughts in the Nura–Sarysu, Esil, and Tobyl–Torgai WMBs of Kazakhstan (Figure 1). Unlike most previous research, primary attention is focused not on individual drought index values, but on evaluating their spatial coherence, identifying hydroclimatic non-stationarity, and analyzing the sequential stages of drought formation at the basin scale.

The objective of this study is a comprehensive assessment of the spatiotemporal variability, spatial coherence, and hydroclimatic non-stationarity of meteorological and hydrological droughts in the Nura–Sarysu, Esil, and Tobyl–Torgai WMBs based on the joint application of SPI, SPEI, and SDI. To achieve this objective, the following tasks were addressed: characterization of the long-term dynamics of meteorological and hydrological droughts; identification of structural shifts and the main stages of hydroclimatic regime transformation; evaluation of the influence of atmospheric precipitation and air temperature on drought formation; and determination of the spatial coherence and relationships between meteorological and hydrological droughts in the studied basins.

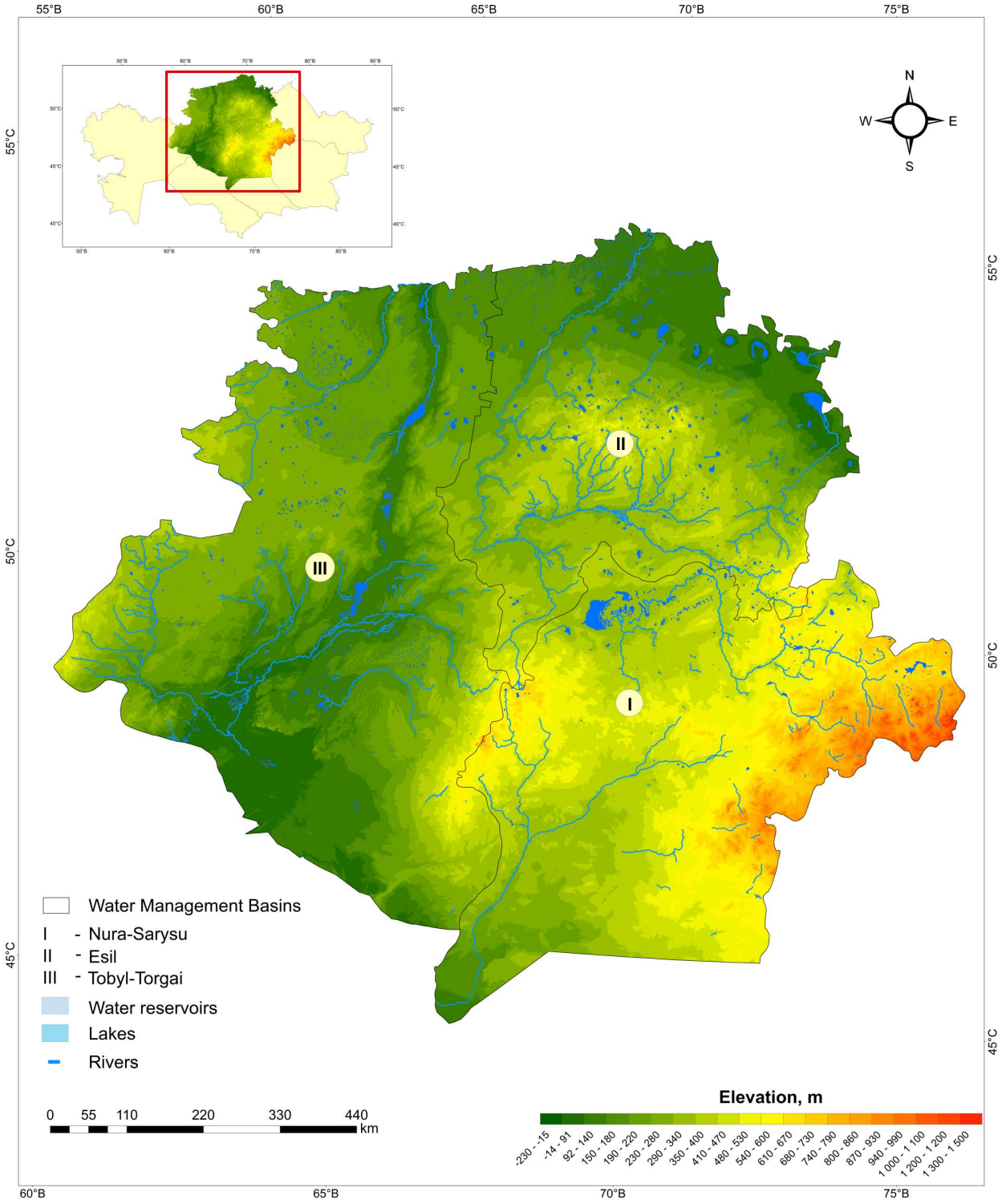

Figure 1. Overview map of the study area.

2. Materials and Methods

2.1. Study Area

The water management basins under investigation are situated in Northern and Central Kazakhstan, accounting for approximately 30% of the national territory.

The Nura–Sarysu WMB predominantly encompasses the Karaganda region, along with portions of the Akmola and Ulytau regions. This territory is characterized as an endorheic (internal drainage) area: the Nura, Kulanotpes, and other watercourses discharge

into terminal lakes, while the Sarysu River basin consists of a system of ephemeral streams. The region features steppe and semi-desert landscapes under a sharply continental climate, with runoff heavily dependent on the spring freshet. The prevailing soils are chestnut and dark chestnut. Water resources from the Nura River are utilized for industrial purposes, municipal supply, and power generation, supporting major urban centers including Karaganda. Agronomically, the basin specializes in the production of cereal and fodder crops, as well as pastoral livestock farming.

The Esil WMB covers Northern Kazakhstan (Akmola and North Kazakhstan regions). Its principal watercourse is the Esil River, a major left-bank tributary of the Ertis River. The basin is distinguished by fertile soils, which have facilitated its development into one of the country's primary grain-producing regions. The basin remains vital for national food security, making sustainable water resource management critical in the face of climatic variability.

The Tobyl–Torgai WMB is located primarily within the Kostanay region, extending partially into the Aktobe and Karaganda regions. The regional climate and flat topography define the characteristics of the hydrographic network, which comprises both intermittent and perennial watercourses. The bulk of the annual runoff is generated during the spring, resulting in brief freshets followed by summer low-flow periods. The river network includes the Tobyl River basin and the Torgai River system; several tributaries of the latter dissipate in topographic depressions. Chernozem and chestnut soils predominate, supporting extensive grain farming and livestock production. A general map of the study area is provided in Figure 1.

The studied water management basins are not undisturbed natural catchments. River flow is regulated to varying degrees by reservoirs and is influenced by water intakes for municipal, industrial, and agricultural use. In the Esil WMB, the main objects of long-term regulation are the Vyacheslavskoye (Astana) and Sergeyevskoye reservoirs; the Vyacheslavskoye Reservoir was filled during 1967–1970, while the Sergeyevskoye Reservoir was commissioned in 1969. In the Tobyl–Torgai WMB, the main long-term flow-regulation structures include the Verkhne-Tobolskoye and Karatomar reservoirs, the latter having been in operation since 1966. In the Nura River WMB, the flow is regulated by a system of reservoirs and ponds; one of the most significant facilities is the Samarkand reservoir, which was reconstructed in 1972–1988. The temporal dynamics of river flow in the studied water basins reflect a combination of natural hydroclimatic processes and water management effects.

2.2. Research Materials

The study used long-term time series of observations on precipitation, air temperature and water discharge obtained from the State Hydrometeorological Network of the Republican State Enterprise 'Kazhydromet' of the Republic of Kazakhstan (http://ecodata.kz:3838/dm_climat_ru/ (accessed on 1 September 2026); https://www.kazhydromet.kz/ru/gidrologiya/ezhegodnye-dannye-o-rezhime-i-resursah-poverhnostnyh-vod-sushi-eds (accessed on 1 September 2026)), which provide sufficiently long and statistically representative observation series.

These datasets were used to calculate drought index series at 3-, 6-, and 12-month timescales. Meteorological drought indices (SPI and SPEI) and the hydrological drought index (SDI) were calculated using the Drought Monitoring Analysis Program (DMAP) software Version 2.1, based on observational data from ground-based meteorological stations and hydrological posts within the study area.

Prior to calculations, the raw data underwent a quality control procedure that included checking time series completeness, identifying anomalies, filling gaps, and verifying the temporal consistency of observations. To ensure accurate temporal comparison between meteorological stations, the graphical representation of the SPI-3 and SPEI-3 time series

was standardized within the overall time interval of 1930–+2024. Periods preceding the start of actual observations at a specific station, as well as intervals with missing data, were left blank and were not interpreted as index values. To ensure comparability of results, only time series satisfying the established criteria were included in the further analysis. The observation periods and main characteristics of the meteorological stations and hydrological posts are presented in Tables 1 and 2.

Table 1. Meteorological stations.

№	Meteorological Station	Elevation, m	Latitude (°N)	Longitude (°E)	Observation Period
		Nura–Sarysu WMB			
1	Aksu–Ayuly	724	48.7680	73.6774	1945–2024
2	Zhana–Arka	489	48.6969	71.6703	1939–2024
3	Bes–Oba	715	49.3456	74.4761	1942–2024
4	Karagandy	552	49.8193	73.1498	1932–2024
5	Korneevka	600	50.2133	74.2682	1959–2024
6	Zhezkazgan	345	47.7728	67.6904	1937–2024
7	Korgalzhyn	331	50.5917	69.9975	1970–2024
8	Zharyk	656	48.8532	72.8371	1936–2024
		Esil WMB			
1	Blagoveshchenka	150	54.3597	66.9801	1938–2024
2	Vozvyshenka	127	54.4326	70.9619	1931–2024
3	Kishkenekol	98	53.6280	72.3315	1960–2024
4	Akkol	383	51.9914	70.9439	1935–2024
5	Ruzaevka	227	52.8224	66.9581	1937–2024
6	Saumalkol	319	53.3094	68.1146	1939–2024
7	Sergeevka	141	53.8833	67.3975	1968–2024
8	Taiynsha	153	53.8636	69.8017	1935–2024
9	Chkalovo	164	53.6246	70.4527	1956–2024
10	Yavlenka	120	54.2917	68.3408	1932–2024
11	Arshaly	426	50.8633	72.1478	1975–2024
12	Atbasar	302	51.8419	68.3636	1931–2024
13	Balkashino	399	52.5281	68.7431	1936–2024
14	Yegindykol	340	51.0522	69.4956	1973–2024
15	Ereimentau	397	51.6125	73.0942	1955–2024
16	Bulaevo	134	54.9111	70.4578	1937–2024
17	Astana	347	51.1500	71.1500	1936–2024
18	Shchuchinsk	393	52.9250	70.2036	1938–2024
		Tobyl–Torgai WMB			
1	Dievskaya	214	52.0089	63.6850	1957–2024
2	Amangeldy	142	50.1986	65.2072	1938–2024
3	Arshalinsky	260	52.7236	61.1403	1956–2024
4	Jetygara	279	52.1925	61.1783	1936–2024
5	Kostanay	151	53.2369	63.7411	1963–2024
6	Kushmurun	110	52.4544	64.5931	1938–2024
7	Tobol	208	52.7033	62.5711	1952–2024
8	Torgai	133	49.6347	63.4822	1932–2024
9	Irgiz	114	48.6194	61.2603	1937–2024
10	Karabutak	229	49.9722	60.1131	1942–2024
11	Komsomolskoye	187	53.7411	62.0517	1940–2024

Table 2. Hydrological posts.

№	Hydrological Post (River—Settlement)	Watershed Area (km^2)	Observation Period	Reconstructed Years
		Nura–Sarysu WMB		
1	Nura—Besoba	1050	1960–2023	1984–1985, 1995
2	Nura—Sheshenkara	8320/13,980	1960–2023	1974, 1996–1998, 2000
3	Nura—Balykty	12,300/17,960	1960–2023	1998–1999, 2022
4	Nura—Koshkarbayeva	45,100/50,760	1960–2023	1994, 2005–2006, 2016–2017
5	Sherubainura—Karamurun	8700	1960–2023	1998–1999
6	Sarysu—Razyezd 189	26,900	1962–2023	1962, 1964, 1995, 1997–1999
7	Zhaman-Sarysu—Atasu	9200	1960–2023	1960–1967, 1970–1975, 1978, 1980, 1992

Table 2. *Cont.*

№	Hydrological Post (River—Settlement)	Watershed Area (km^2)	Observation Period	Reconstructed Years
		Esil WMB		
1	Silety—Prirechnoye	2850	1957–2023	1960, 1962, 1980, 1998, 1999
2	Silety—Izobilnoye	24,450	1957–2023	1965–1967, 1971, 1972, 1984, 1993, 1997–2000, 2004, 2005, 2007
3	Shagalaly—Pavlovka	1750	1939–2023	1981, 1983, 1984, 1986–1990, 1992, 1995, 2001, 2003, 2006–2008, 2011
4	Shagalaly—Severnoye	5040/8360	1973–2023	1992, 1994–2010, 2013
5	Moiyldy—Nikolayevka	472	1973–2023	1973, 1988, 1989, 1991, 1994, 1998–2000
6	Esil—Turgen	3240	1974–2023	1974, 2009
7	Kalkutan—Kalkutan	16,500	1936–2023	1956, 2008, 2010, 2011
8	Zhabay—Balkashino	922	1937–2023	1992, 1998, 1999, 2003, 2004, 2008
9	Zhabay—Atbasar	8530	1936–2023	1941–1943, 1946, 1956, 1971
10	Akkanburlyk—Vozvyshenka	5620/6250	1936–2023	1941–1950, 1962, 1963, 1980–1988, 1990–2002, 2004, 2006
11	Imanburlyk—Sokolovka	3970/4070	1950–2023	1981, 1984, 1996–2003
		Tobyl–Torgai WMB		
1	Tobyl—Akkarga	2820	1959–2018	1977–1978, 1982–1986, 1990–2002, 2009, 2019–2022
2	Tobyl—Grishenka	13,100/13,400	1937–2023	1977, 1979–1982, 1987, 1991–1997
3	Tobyl—Kostanay	28,000/44,800	1931–2023	1931, 1971, 1989, 1994, 1998
4	Ayat—Varvarinka	9020/10,300	1952–2023	1974, 1976, 1981–1983, 1988, 1990, 1992
5	Togyzak—Togyzak	5970/7970	1936–2023	1963, 1966, 1976, 1984, 1987–1988, 1990–1991, 1994–1996, 1998–2002
6	Ubagan—Aksuat	17,200/22,300	1938–2023	1945–1957, 2006, 2008–2012, 2018–2019
7	Damdy—Damdy	1850	1955–2023	1957–1960, 1963–2005
8	Torgai—Tusum	52,300/56,500	1940–2023	1982, 1984, 1986, 1989, 2007–2009
9	Karatorgai—Urpek	14,800/15,000	1941–2023	1964, 1969, 1974, 1976, 1977, 1981, 1994, 1996–2000, 2006–2009
10	Sarytorgai—Sarytorgaiskiy	5600	1960–2023	1963, 1980–1981, 1983–1985, 2008, 2013–2015
11	Yrgyz—Shenbertal	22,700/26,800	1961–2023	1961, 1966, 1988, 1995, 1997–2005, 2014–2015

Note: For river catchments containing endorheic (closed-drainage) areas, two values of the catchment area are provided: the numerator indicates the effective catchment area, while the denominator indicates the total catchment area.

Potential evapotranspiration was calculated using a set of meteorological variables (air temperature (mean, minimum, maximum), precipitation, wind, radiation, and relative humidity) required for the application of the FAO-56 Penman–Monteith method. The calculated PET values were used as input data for the subsequent determination of SPEI in the DMAP software (https://agrimetsoft.onfastspring.com/ (accessed on 1 September 2026)).

SPI and SPEI standardization period. In the main analysis, SPI-3 and SPEI-3 were calculated separately for each weather station using the full available observation period shown in Table 1. The parameters of the probability distributions were estimated relative to the actual period for each station. Since the start dates of observations varied, the duration of the standardization period was also inconsistent. This circumstance was taken into account when interpreting inter-station differences. The absolute values of the indices were not considered to be directly equivalent measures of the long-term climatic background at different stations. Spatial consistency was assessed primarily based on the simultaneous attainment of a single categorical drought threshold (SPI-3/SPEI-3 ≤ -1.0) and the proportion of stations in the basin that met this condition during the corresponding time step.

The spatial distribution of these meteorological stations and hydrological posts is illustrated in Figure 2.

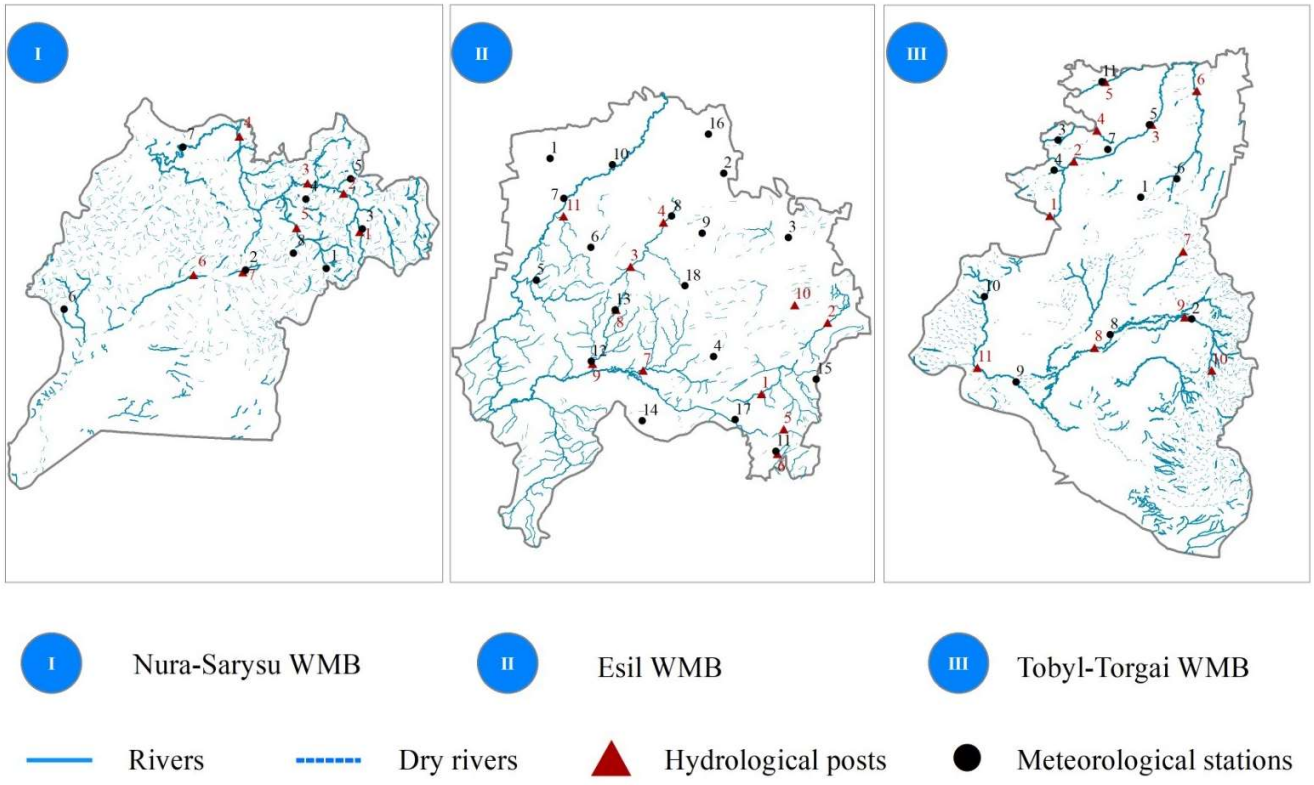

Figure 2. Schematic map of the location of hydrological posts and meteorological stations following the numbering shown in Tables 1 and 2.

2.3. Research Methods

2.3.1. Reconstruction of Streamflow Time Series

Hydrological observation records are often characterized by unequal record lengths, missing observations, and inhomogeneities resulting from both limited monitoring coverage and anthropogenic alterations of river regimes. To ensure the consistency and completeness of the dataset, missing values and shortened observation series were reconstructed using the hydrological analogy method. This approach relies on data from analog catchments exhibiting comparable physiographic and climatic conditions governing runoff formation.

The selection of analog rivers was based on the following criteria: (i) geographical proximity and similarity of climatic conditions; (ii) synchronous long-term runoff variability; (iii) comparable hydrogeological conditions controlling runoff generation; (iv) similarity in catchment characteristics, including drainage area and mean basin elevation; (v) a sufficiently long period of overlapping observations; and (vi) the absence of substantial anthropogenic impacts on the flow regime during the reference period.

For the period of joint observations, the correlation coefficient was estimated; in the dependencies used, the values of the correlation coefficient were mainly in the range of 0.70–0.97.

To assess the possible impact of reconstruction on the results of structural change analysis, for each hydrological series used, the years of statistically significant SDI-12 change points were compared with the years actually restored. Additionally, the distance in years between the breakpoint and the nearest restored value was determined. The case when the breakpoint fell on the restored year was considered a direct coincidence; the cases of the location of the breakpoint within ± 1 year of the restored value were considered close.

The reconstruction procedure was performed using statistically significant relationships between streamflow records at the target and analog gauging stations. Application

of the hydrological analogy method enabled the development of homogeneous and continuous discharge time series, providing a reliable basis for the subsequent calculation of hydrological drought indices and the assessment of their long-term variability [19].

2.3.2. Time Series Homogeneity Assessment

In the present study, the following statistical methods were employed to analyze the homogeneity of the time series: The Buishand Range Test was applied to detect abrupt step changes in the mean values. The Cumulative Sum (CUSUM) method was utilized to assess systematic biases in the mean and to visualize the specific timing of hydroclimatic regime shifts.

The Standard Normal Homogeneity Test (SNHT) developed by [20] was applied to identify statistically significant shifts in the mean level of the hydrological time series. The test is based on comparing a standardized candidate series with a homogeneous reference series and evaluating possible changes in the mean at each time step. For each potential change point (k), the standardized series is divided into two segments, and the SNHT statistic is calculated from the squared deviations of the mean values of these segments from the overall mean. The maximum value of the statistic, (T_0), is used to identify the most probable change point. A statistically significant (T_0) indicates a departure from homogeneity, while the corresponding time step is considered the location of a statistically significant structural shift in the time series [21,22]. In this study, the SNHT results were interpreted as evidence of temporal structural changes or change points in individual streamflow series rather than as a general measure of non-stationarity.

The non-parametric Pettitt test is employed to detect a single change-point within a time series. This method is based on Mann–Whitney rank-based statistics and does not require the assumption of a normal distribution. The test statistic U_t is determined through a sequential comparison of two subsamples [23] (Equation (1)):

$$U_t = 2\sum R_i - t \times (n+1) \quad (1)$$

The moment in time at which U_t reaches its maximum value is interpreted as the most probable point of a structural shift. Statistical significance is assessed at the $\alpha = 0.05$ level.

The Buishand Range Test is employed to verify the hypothesis regarding the homogeneity of the time series mean. This method is based on an analysis of the cumulative deviations from the mean value [24] (Equation (2)):

$$S_k = \sum_{i=1}^{k} (X_i - \overline{X}) \quad (2)$$

where X_i is the SDI value; $\overline{X}$ is the mean value for the entire observation period. The calculation of the adjusted range of accumulated deviations allows for identifying the presence of a jump-like change in the average level. Statistical significance is evaluated at the $\alpha = 0.05$ level.

The CUSUM method is employed to detect systematic deviations of time series from the mean level and to graphically identify potential change-points. In a homogeneous series, the CUSUM curve fluctuates around the zero axis. A change in the slope of the curve or a sustained deviation from the zero line is interpreted as an indication of a structural transformation in the hydrological regime [25].

The application of multiple statistical tests is necessitated by the need to enhance the robustness of the conclusions and to eliminate potential methodological bias in the results. The convergence of change-points identified by different methods is regarded as statistically sound evidence of a shift in the streamflow drought regime.

In this study, the results of the Pettitt, Buishand, SNHT and CUSUM tests were interpreted as evidence of statistically significant structural changes and potential regime-switching points in the time series. The presence of such a transition point was not considered an independent quantitative measure of process non-stationarity; accordingly, the proportion of series with significant transition points was used exclusively as a measure of the prevalence of structural shifts within the respective river basin.

Statistically significant points of change identified by the Pettitt, Buishand, SNHT and CUSUM tests were interpreted in this study as structural shifts in the time series, but not as independent evidence of a change in the hydroclimatic regime. In addition to climatic and hydrological factors, statistical heterogeneity in long instrumental time series may potentially be associated with changes in the observation network, including the relocation of observation sites, replacement of instruments, or changes in measurement procedures. Since complete historical metadata on such changes for all stations and observation points over the entire study period were unavailable, the physical interpretation of individual points of change was conducted with caution. Regional climatic interpretation was considered only when there was temporal consistency among the structural shifts in several independent time series and their correspondence to changes in key climatic characteristics.

2.3.3. Accounting for Serial Correlation and Multiple Testing

Since SPI-3 and SPEI-3 are calculated using overlapping three-month intervals, consecutive monthly index values are not statistically independent. To quantitatively assess serial dependence, the first-order autocorrelation coefficient (r_1) between consecutive monthly values was calculated for each time series. Only pairs of adjacent calendar months with available index values were included in the calculation. Due to the large number of statistical tests, the Benjamini–Hochberg procedure was additionally applied to control the false discovery rate (FDR). The correction was performed separately within each homogeneous group "timescale × statistical test" at $q < 0.05$. As an additional robustness check, a global FDR correction was also calculated for all available numerical *p*-values. Structural changes were interpreted as the most robust when statistical significance was retained after FDR correction, and the change was confirmed by several independent change-point tests.

2.3.4. Calculation of the Standardized Precipitation Index

The Standardized Precipitation Index was developed by [26]. This index enables the assessment of precipitation deviations from the climatological normal across various timescales and is widely utilized for the characterization of droughts of varying durations. The initial monthly precipitation totals are aggregated over k-month timescales (e.g., SPI-1, SPI-3, SPI-6, SPI-9, and SPI-12) (Equation (3)):

$$X_t = \sum_{i=0}^{k-1} P_{t-i} \tag{3}$$

where P_t is the monthly precipitation total and X_t represents the accumulated precipitation over a k-month period. Calculations are conducted independently for each calendar month to account for the seasonal variability in precipitation distribution.

The distribution of accumulated precipitation is assumed to follow a gamma distribution as shown in Equation (4):

$$g(x) = \frac{1}{\beta^{\alpha}\Gamma(\alpha)} x^{\alpha-1} e^{-x/\beta} \tag{4}$$

where α is the shape parameter, β is the scale parameter, and $\Gamma(\alpha)$ is the gamma function.

Distribution parameters are estimated using the Maximum Likelihood Estimation (MLE) method. Since the gamma distribution is undefined for $x = 0$, the mixed probability of zero precipitation is incorporated (Equation (5)):

$$H(x) = q + (1 - q)G(x) \quad (5)$$

where q is the proportion of zero values and $G(x)$ is the cumulative gamma distribution function.

The resulting cumulative probability $H(x)$ is then transformed into the standard normal distribution (Equation (6)):

$$SPI = \phi^{-1}(H(x)) \quad (6)$$

where ϕ^{-1} is the inverse cumulative standard normal distribution function.

Consequently, the resulting SPI has a mean (expected value) close to zero and a standard deviation of one (Table 3).

Table 3. Classification of drought conditions according to the SPI.

SPI Value Intervals	Characterization of the Dryness Category of the Territory
≥2.00	Extremely wet
1.50 to 1.99	Very wet
1.00 to 1.49	Moderately wet
−0.99 to 0.99	Near normal
−1.00 to −1.49	Moderately dry
−1.50 to −1.99	Severely dry
≤−2.00	Extremely dry

2.3.5. Calculation of the Standardized Precipitation Evapotranspiration Index

Potential evapotranspiration (PET) was calculated separately in Python 3.14.7 using the FAO-56 Penman–Monteith equation, recommended by the Food and Agriculture Organization (FAO), Rome, Italy, of the United Nations (New York, NY, USA), for reference evapotranspiration [27]. The calculated PET values were exported to a separate file and imported into the Drought Monitoring Analysis Program (DMAP v2.0, AgriMetSoft (Ames, IA, USA)), where, together with precipitation time series, they were used for the automated calculation of the SPEI. In this study, the SPEI mode utilizing pre-calculated PET values was applied, rather than the 'SPEI by T' mode, which computes PET directly within the software using the Thornthwaite method. DMAP was used exclusively as a computational platform to implement the original SPEI algorithm proposed by [28].

Based on the monthly difference between precipitation and potential evapotranspiration, the software calculated the climatic water balance (Equation (7)):

$$D_t = P_t - PET_t \quad (7)$$

where P_t is the monthly precipitation total, PET_t is the Potential Evapotranspiration, and D_t represents the moisture deficit or surplus.

To analyze droughts of varying durations, the D_t values are aggregated over k-month timescales (Equation (8)):

$$X_t = \sum_{i=0}^{k-1} D_{t-i} \quad (8)$$

where X_t is the accumulated water balance for the period k. Calculations are performed separately for each calendar month to account for seasonal variability.

The obtained X_t values are approximated by a three-parameter distribution that well describes the variability of the water balance, as shown in Equation (9).

$$F(x) = \left[1 + \left(\frac{\propto}{x - \gamma}\right)^{\beta}\right]^{-1} \quad (9)$$

where α is the scale parameter, β is the shape parameter, and γ is the location parameter. The parameters of the distribution are estimated using the L-moments method.

The resulting cumulative probability $F(x)$ is then transformed into the standard normal distribution (Equation (10)):

$$SPEI = \phi^{-1}(F(x)) \quad (10)$$

where ϕ^{-1} is the inverse function of the standard normal distribution. Unlike SPI, the SPEI reflects the joint influence of precipitation and air temperature. In conditions of rising air temperature, negative SPEI values can intensify even without significant changes in precipitation, which allows for identifying temperature-driven intensification of drought, especially relevant for arid and semi-arid regions.

2.3.6. Assessment of the Spatial Coherence of Drought

To quantitatively assess the spatial consistency of meteorological drought, the proportion of weather stations in the corresponding watershed that simultaneously exhibited drought conditions was calculated for each time step:

$$SC_t = \frac{N_{d,t}}{N_{a,t}} \times 100\% \quad (11)$$

where SC_t is the spatial consistency of drought at time t, in percent; $N_{d,t}$ is the number of weather stations with SPI-3 or SPEI-3 values ≤ -1.0; $N_{a,t}$ is the number of stations in the corresponding basin for which data were available at the time in question.

An SPI-3/SPEI-3 ≤ -1.0 threshold corresponds to the onset of moderate drought according to the classification adopted in this study. Stations for which data were missing at a specific time step were not included in the denominator. This approach allows for variations in the duration of observation series and changes in the composition of the observation network over time. For each identified drought episode, the maximum value of SC_t was determined; when interpreting the results, the actual ratio n/N was taken into account alongside the spatial consistency value, where n is the number of stations experiencing drought conditions, and N is the number of stations with available observations for the corresponding time step.

Using the relative proportion of stations that simultaneously exceed a single drought threshold allows us to assess the spatial synchrony of events without directly comparing the absolute SPI-3 and SPEI-3 values between stations, which are calculated relative to climatic periods of varying durations.

2.3.7. Calculation of the Streamflow Drought Index

The assessment of hydrological drought was conducted using the Streamflow Drought Index (SDI), as proposed by [29]. This index is based on an analysis of accumulated streamflow volumes over a specified aggregation interval (seasonal or annual) and reflects standardized deviations from long-term average conditions (Equation (11)):

$$SDI_{i,k} = \frac{W_{i,k} - \overline{W}_k}{\sigma_k} \quad (12)$$

where $\overline{W}_k$ is the long-term mean of the accumulated runoff volume, and σ_k is the standard deviation. The resulting time series characterizes the intensity and duration of hydrological drought and enables the comparison of water availability across different periods (Table 4).

Table 4. SDI values for drought severity classification.

SDI Value	Description
≥2.0	Extremely Wet
1.99–1.50	Very Wet
1.49–1.00	Moderately Wet
0.99–−0.99	Near Normal
−1.00–−1.49	Moderately Dry
−1.5–−2.0	Severe Dry
SDI < −2.0	Extremely Dry

The SDI reflects the integral response of the hydrological system to both climatic and anthropogenic impacts. It facilitates the analysis of the duration and intensity of hydrological droughts, long-term variability in water availability, and the synchronicity of dry periods within a river basin. Unlike meteorological indices such as SPI and SPEI, the SDI characterizes the actual state of water resources and accounts for the influence of runoff formation processes, including snow storage, flow regulation, and water consumption.

The selection of time scales for SPI, SPEI, and SDI was determined by the characteristics of different drought types and the objectives of the study. Drought propagation is a sequential process in which an initial precipitation deficit leads to the formation of a meteorological drought, subsequently manifests as a reduction in soil moisture reserves, developing into an agricultural drought, and, if the moisture deficit persists over an extended period, causes the depletion of surface and groundwater resources, resulting in a hydrological drought. Thus, different types of droughts are characterized by varying rates of development and differing hydrological inertia.

In accordance with this concept, the SPI-3 was used to characterize short-term precipitation deficits, reflecting the initial stage of drought development. The SPEI-3, taking into account the effect of potential evapotranspiration, was applied to assess short-term changes in the climatic water balance during the growing season. The SDI-12 was used to characterize hydrological drought, as the 12-month time scale allows for the cumulative effect of prolonged moisture deficits to be taken into account and reflects the integrated response of the river basin, including river runoff depletion. This approach aligns with the concept of sequential drought propagation and allows for the analysis of various stages in the formation of water resource deficits.

In this study, SDI-12 was used to characterize the integral state of hydrological drought on an annual timescale. Due to the difference in timescales between SPI-3/SPEI-3 and SDI-12, a quantitative assessment of the time it takes for meteorological drought to propagate into hydrological drought (drought propagation lag) was not performed.

Additionally, the relationship between the catchment area and the characteristics of hydrological drought was analyzed for 29 hydrological posts of the three studied water basins. For catchments containing drainless areas and characterized by two area values, the effective catchment area corresponding to the numerator in Table 2 was used.

For each hydrological post, three characteristics were determined using the SDI-12 time series: the standard deviation of SDI-12, the minimum value of SDI-12, and the frequency of hydrological drought, defined as the proportion of observations with SDI-12 < −1.0. The relationship of each characteristic to the catchment area was estimated using Spearman's rank correlation coefficient [30]. The choice of a nonparametric coefficient is due to the wide range of areas of the studied catchments and the absence of an assumption about the linear nature of the dependence.

3. Results

The results are organized to evaluate drought dynamics from three complementary perspectives: temporal structural shifts, meteorological drought variability, and hydrologi-

cal response. First, the homogeneity analysis identifies structural shifts in the SPI, SPEI, and SDI time series, providing evidence of changes in the statistical behavior of drought regimes. Second, the SPI and SPEI results are used to distinguish precipitation-driven drought variability from drought intensification associated with atmospheric water demand. Third, the SDI analysis assesses how meteorological anomalies are transferred to streamflow deficits, considering the delayed and integrated response of river basins. This structure allows drought evolution to be interpreted not only in terms of isolated index values, but also as a sequence of basin-scale hydroclimatic responses involving atmospheric forcing, evaporative demand, and runoff generation processes.

Across the three water management basins, drought behavior is characterized by a combination of recurrent regional episodes and spatially differentiated basin responses. Therefore, the interpretation of the results focuses on three aspects: the timing of structural shifts, the degree of spatial coherence of dry and wet phases, and the consistency or divergence between meteorological and hydrological drought signals. This framework provides the basis for identifying whether drought episodes correspond to local anomalies or to broader hydroclimatic reorganizations affecting large parts of northern and central Kazakhstan.

3.1. Changes in Main Climatic Factors

3.1.1. Air Temperature

The Mann–Kendall test and Sen's slope estimator indicate a statistically significant warming trend across all meteorological stations and seasons (Table S1). Mean annual air temperature increased by 0.25–0.38 °C/decade ($p < 0.001$), with the strongest warming observed at the Zhetikara MS and the weakest at the Atbasar MS.

Seasonal warming was most pronounced in spring (0.33–0.45 °C/decade) and winter (0.22–0.44 °C/decade), whereas summer exhibited the weakest trends (0.04–0.23 °C/decade), with several stations showing non-significant changes. Overall, the results demonstrate a spatially coherent warming pattern across the study area.

The Pettitt test identified significant shifts in seasonal and annual temperature series (Table S2). Most annual change points occurred during 1976–1987, while winter shifts clustered around 1978–1980 and spring shifts mainly occurred in the late 1990s. These results indicate a non-synchronous but persistent transformation of the regional temperature regime.

3.1.2. Precipitation

Precipitation changes were considerably more heterogeneous than temperature changes (Table S3). The strongest positive trends occurred in winter (1.8–7.4 mm/decade) and annual totals (2.0–21.1 mm/decade), whereas statistically significant summer trends were absent. A significant decrease in annual precipitation was detected only at the Bes-Oba MS.

According to the Pettitt test, precipitation change points were spatially inconsistent (Table S4). Significant shifts were most frequently observed in winter and annual series, while summer precipitation exhibited no statistically significant structural changes. Overall, precipitation variability showed substantially greater spatial and temporal heterogeneity than temperature.

3.1.3. Atmospheric Circulation

The circulation analysis revealed statistically significant long-term changes in large-scale atmospheric circulation (Table 5). The frequency of the zonal circulation type (W) increased, whereas the easterly type (E) decreased. Positive winter and spring trends were also identified for the AO and NAO indices.

Table 5. Results of the Mann–Kendall test and Sen's slope estimator for atmospheric circulation indices.

Circulation Index	Winter	Spring	Summer	Autumn	Annual
AO	0.014 *	0.011 **	0.001 ns	0.003 ns	0.007 **
NAO	0.017 ***	0.006 *	−0.007 ns	−0.005 ns	0.003 ns
E	−0.261 **	−0.280 ***	−0.037 ns	0.000 ns	−0.518 **
W	0.299 ***	0.196 ***	0.078 ns	0.179 **	0.672 ***
C	−0.030 ns	0.103 +	−0.031 ns	−0.125 *	−0.059 ns

Note: ***—$p < 0.001$; **—$p < 0.01$; *—$p < 0.05$; + $p < 0.10$; ns—statistically non-significant.

Pettitt test results indicate that the principal circulation regime shifts occurred during the 1980s, particularly for the W and E circulation forms (Table 6). These changes broadly coincide with the timing of the detected temperature and precipitation shifts.

Table 6. Change points in seasonal and annual time series of circulation indices identified using the Pettitt test.

Circulation Index	Winter	Spring	Summer	Autumn	Annual
AO	1988 *	1984 +	1969 ns	1968 ns	1987 **
NAO	1980 ***	1981 +	1996 ns	1993 ns	1970 ns
Vangengeim_W	1987 ***	1987 ***	1984 +	1993 *	1985 ***
Vangengeim_E	1986 ***	1989 ***	1990 +	1994 ns	1989 ***
Vangengeim_C	2007 ns	2003 *	1971 ns	1973 *	1971 *

Note: ***—$p < 0.001$; **—$p < 0.01$; *—$p < 0.05$; + $p < 0.10$; ns—statistically non-significant.

The strengthening of zonal circulation likely enhanced the transport of warm and moist Atlantic air masses into Northern and Central Kazakhstan, contributing to the observed warming and increased cold-season precipitation. The absence of significant summer circulation changes is consistent with the lack of robust trends in summer precipitation, suggesting that atmospheric circulation was an important driver of the detected climatic changes.

3.2. Time Series Homogeneity Assessment

Under contemporary climate variability, the analysis of drought and streamflow index time series requires careful consideration of potential changes in their statistical structure. Long-term climatic and hydrological series may contain statistically significant structural shifts associated with changes in the mean or other statistical characteristics of the series. However, the detection of a change point alone does not establish its physical cause or demonstrate a change in the hydroclimatic regime. Therefore, in this study, the analysis focused on identifying statistically significant structural shifts and their spatial and temporal distribution rather than interpreting individual change points as unequivocal evidence of climatic or hydrological regime changes.

To identify statistically significant structural shifts in the long-term drought and streamflow index series, the non-parametric Pettitt, Buishand, SNHT, and CUSUM tests were applied. The use of several complementary change-point tests increases the robustness of the assessment because the methods differ in their sensitivity to changes in the mean and other characteristics of time series. The results of these tests were interpreted as evidence of statistically significant structural shifts or change points in individual time series. The proportion of series containing significant change points was used to characterize the prevalence of structural shifts within each WMB and was not interpreted as an independent quantitative measure of non-stationarity.

Analysis of long-term drought index time series revealed statistically significant changes in their temporal structure. The identified points of change are considered, first and foremost, as statistical indicators of heterogeneity in the corresponding time series. Their possible connection to changes in regional hydroclimatic conditions was assessed taking

into account the temporal consistency between independent time series and changes in key climatic factors; no causal interpretation of individual points of change was performed.

3.2.1. Assessment of SPI Time Series Homogeneity

The analysis of SPI-3 time series revealed statistically significant structural shifts in short-term precipitation-related moisture conditions across the study area (Table S5). Significant change points were identified in 88% of stations in the Nura–Sarysu WMB, 72% in the Esil WMB, and 55% in the Tobyl–Torgai WMB, indicating substantial spatial differences in the prevalence of temporal structural changes.

Among the three basins, the Esil WMB demonstrated the greatest temporal and spatial consistency of the detected change points, with a considerable proportion occurring during the 1960s–1970s. In the Nura–Sarysu WMB, significant change points were distributed over a broader period, from the 1950s to the early 2000s. The Tobyl–Torgai WMB exhibited fewer significant change points and greater spatial heterogeneity in their timing. These differences indicate that the temporal structure of SPI-3 series varies among the three basins, with different degrees of spatial consistency in the detected changes.

Overall, approximately 60% of the SPI-3 time series contained statistically significant structural shifts. The highest concentration of change points occurred during the 1950s–1960s, the late 1960s–1970s, and the late 1990s–early 2000s. The temporal clustering of structural shifts across several independent time series indicates regionally consistent changes in short-term moisture conditions during these periods. However, the coincidence of change points does not by itself establish their climatic origin. A possible climatic interpretation is supported only where temporally consistent structural shifts occur across several independent series and correspond to concurrent changes in relevant climatic characteristics.

3.2.2. Assessment of SPEI Time Series Homogeneity

The analysis of SPEI-3 time series identified statistically significant structural shifts across the study area (Table S6). Significant change points were detected in 62% of stations within the Nura–Sarysu WMB, 56% within the Esil WMB, and 27% within the Tobyl–Torgai WMB. These differences indicate substantial spatial variability in the prevalence and timing of structural shifts in the drought index series.

The Esil WMB exhibited the highest spatial consistency, with a large proportion of change points concentrated during 1955–1977. In the Nura–Sarysu WMB, the detected change points were distributed across several periods, indicating a multi-stage pattern of temporal structural changes. The Tobyl–Torgai WMB showed the lowest proportion of series with significant change points and the greatest spatial heterogeneity in their timing. These differences demonstrate that the statistical structure of SPEI-3 series changed at different times and with different spatial consistency across the three basins.

Overall, approximately 40% of the SPEI-3 time series contained statistically significant structural shifts. The highest concentrations of change points were identified during the 1950s–1960s, 1965–1977, and the late 1980s–early 2000s. The temporal coincidence of structural shifts across several independent series suggests regionally consistent changes in drought-related hydroclimatic conditions during these periods. Their correspondence with changes in air temperature and other climatic characteristics may indicate a possible climatic contribution; however, change-point analysis alone does not permit formal attribution of these structural shifts to increasing temperature, evaporative demand, or other individual climatic drivers.

3.2.3. Comparative Analysis of SPI-3 and SPEI-3

Analysis of the SPI-3 time series revealed widespread statistically significant structural shifts, the severity of which varied among the basins studied. In the Nura–Sarysu WMB, significant inflection points were identified for 88% of the analyzed series; in the Esil WMB,

for 72%; and in the Tobyl-Torgay WMB, for 55% (Table 7). Overall, statistically significant structural changes were identified in approximately 60% of the analyzed SPI-3 time series. The points of change were most frequently concentrated in the 1950s–1960s, the late 1960s–1970s, and the late 1990s–early 2000s. The results indicate temporal heterogeneity in the structure of the SPI-3 time series; however, they are not considered, in and of themselves, to be a quantitative measure of the nonstationarity of the climatic process.

Table 7. Proportion of SPI-3 and SPEI-3 time series with statistically significant structural shifts in the studied water management basins.

Water Management Basin	SPI-3 (Share of Structural Shifts), %	SPEI-3 (Share of Structural Shifts), %	Difference, %
Nura–Sarysu	88	62	−25
Esil	72	56	−17
Tobyl–Torgai	55	27	−28
Study area *	70	49	−22

Note: * For the study area, values are calculated as a weighted proportion, defined as the ratio of the total number of meteorological stations with statistically significant structural shifts to the total number of stations. This method avoids bias caused by the unequal number of stations across different water management basins.

For SPEI-3, statistically significant structural shifts were also identified in all studied basins; however, the proportion of affected time series was lower than for SPI-3. Significant transition points were identified for 62% of the Nura–Sarysu, 56% of the Esil, and 27% of the Tobyl-Torgay WMBs. The results indicate a less widespread occurrence of detectable SPEI-3 structural changes compared to SPI-3, particularly in the Tobyl-Torgay WMB.

This pattern highlights the increasing influence of rising air temperature and potential evapotranspiration on drought conditions in the more arid parts of the study area. A comparison of the identified periods of change is presented in Table 8.

The identified differences in the number and timing of structural changes in SPI-3 and SPEI-3 indicate different statistical responses of the two indices to long-term climate variability. However, since SPEI integrates the combined influence of precipitation and potential evapotranspiration through the climatic water balance, differences between SPI and SPEI alone do not allow the contributions of precipitation and atmospheric evaporative demand to be quantitatively separated. Therefore, the obtained results characterize differences in the behavior of the indices but are not considered evidence of the dominant role of either component of the climatic water balance.

Table 8. Comparison of temporal stages.

Period	SPI-3	SPEI-3
1950–1960	Pronounced	Pronounced
1965–1977	Main peak of structural shifts (breaks)	Pronounced, but weaker
1990–2000	Secondary stage	More pronounced

3.2.4. Assessment of SDI Time Series Homogeneity

The analysis of SDI-12 time series revealed statistically significant structural shifts in the hydrological series of the studied river basins (Table S7). Based on the change points identified consistently by the applied statistical tests, most hydrological posts in the Nura–Sarysu and Esil WMBs showed positive changes in mean SDI values, whereas the Tobyl–Torgai WMB demonstrated a more heterogeneous pattern, including both positive and negative shifts. These results indicate differences in the direction and spatial consistency of temporal structural changes in streamflow conditions among the three WMBs.

The highest concentration of statistically significant change points was identified during 1976–1981, representing the most spatially coherent period of structural change,

followed by 1988–1993, when the detected changes were more spatially localized, and 2009–2012. The temporal coincidence of structural shifts across several independent hydrological series during these periods indicates regionally consistent changes in the statistical characteristics of streamflow. Their coincidence with periods of changes in temperature, precipitation, and other climatic characteristics may point to a possible relationship with regional hydroclimatic variability. Nevertheless, such temporal correspondence is not sufficient to establish a causal relationship.

The identified structural changes in SDI characterize a significant temporal heterogeneity in the hydrological series of the studied basins. Their temporary coincidence with individual periods of changes in temperature, precipitation, and regional climatic conditions indicates a possible role of climate variability. At the same time, the rivers under study are characterized by varying degrees of regulation of runoff and economic use of water; therefore, the identified SDI change points cannot be unambiguously attributed solely to climatic effects. The results obtained should be interpreted as a reflection of the combined influence of hydroclimatic conditions, features of runoff formation, and water management regulation.

Further verification of the impact of time series reconstruction showed that statistically significant SDI-12 change points did not coincide exactly with the actually reconstructed flow years. For most stations, significant structural changes were offset from the nearest reconstructed value by several years or more.

At the same time, isolated cases of a close temporary location were identified. For Shagalaly Pavlovka, the change point of 2009 was immediately after the reconstructed value of 2008; for Tobyl–Akkarga, the change point of 1979 followed immediately after the reconstructed value of 1978. These cases were considered potentially more sensitive to the restoration procedure and were not used as independent evidence of a change in the hydrological regime. In other ranks, the time division was significantly greater. For example, the 2011 breakpoint for Nura–Sheshenkara was 11 years from the nearest restored year, for Nura–Besoba it was 16 years, and the 2012 breakpoint for Sarysu–Razyezd No. 189 was 13 years from the nearest restored value.

3.3. Assessment of Serial Correlation and Robustness of Statistical Significance

Analysis of consecutive monthly values confirmed pronounced positive autocorrelation in SPI-3 and SPEI-3 associated with the use of overlapping three-month intervals. For the SPI-3 time series, the median first-order autocorrelation coefficient was r1 = 0.701, with a range of 0.640–0.769. For the SPEI-3 time series, the median was r1 = 0.711, with a range of 0.635–0.758. Statistically significant lag-1 autocorrelation ($p < 0.05$) was identified in all analyzed time series. Differences between basins were small. The median r1 values for SPI-3 were 0.700 in the Nura–Sarysu WMB, 0.710 in the Esil WMB, and 0.698 in the Tobyl–Torgai WMB; the corresponding values for SPEI-3 were 0.704, 0.709, and 0.714. Application of the Benjamini–Hochberg FDR correction showed that the main structure of statistically significant change points was preserved. For the three-month timescale, after correction, 95.2% of the initially significant Buishand results, 95.1% of the initially significant CUSUM results, and 87.5% of the initially significant Pettitt results remained significant. Thus, the correction for multiple testing slightly reduced the number of statistically significant results but did not change the overall conclusion regarding the presence of structural changes in a substantial proportion of the studied time series.

3.4. Standardized Precipitation Index

Under conditions of intensifying climatic variability and the increasing frequency of extreme hydrometeorological events, the quantitative assessment of arid and excessively wet periods is of particular relevance. For the diagnosis of meteorological drought, the

standardized precipitation index is widely applied, as it allows for the evaluation of precipitation deviations from long-term climatic conditions across various time scales.

This index is based exclusively on precipitation data, which ensures its versatility, the comparability of results across different climatic regions, and the possibility of analyzing both short-term and long-term changes in moisture conditions. The use of this index enables identification of the duration, intensity, and frequency of dry periods, as well as assessment of the spatiotemporal variability of atmospheric moisture.

The SPI-3 time series reveal pronounced interannual variability in short-term moisture conditions across the Nura–Sarysu, Esil, and Tobyl–Torgai WMBs, with recurrent alternation of dry and wet periods throughout the observation records (Figures 3 and S1–S3). Drought conditions (SPI ≤ -1.0) account for approximately 16% of observations in the Nura–Sarysu WMB and 17% in the Esil WMB, while severe droughts (SPI ≤ -1.5) occur in approximately 7% and 8%, respectively. Extreme droughts (SPI ≤ -2.0) account for about 3% of observations in both basins. In the Tobyl–Torgai WMB, the SPI-3 series also demonstrate recurrent drought episodes, although their magnitude and spatial expression vary more strongly among meteorological stations.

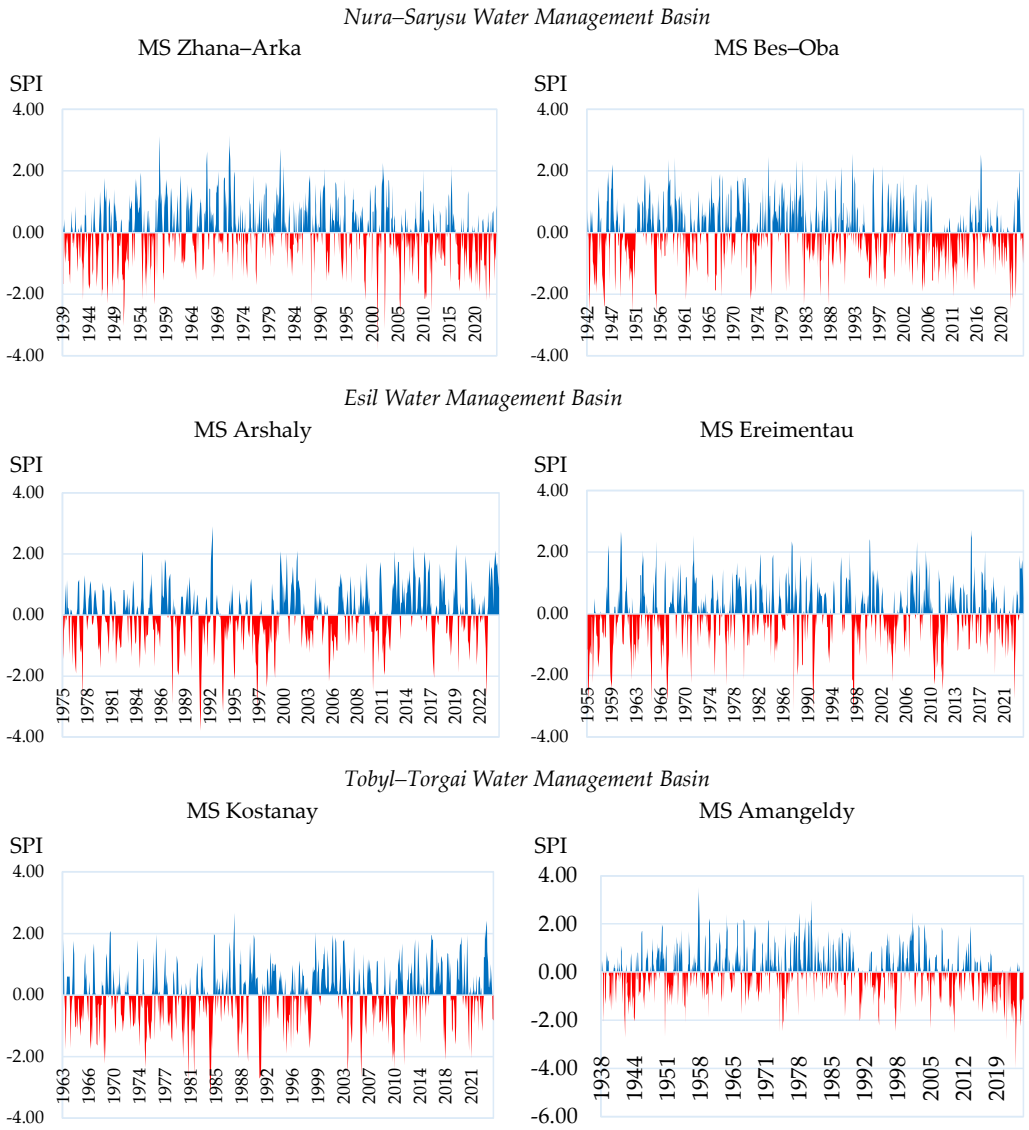

Figure 3. Long-term dynamics of the standardized precipitation index SPI-3 at the main meteorological stations of the study area.

The three Water Management Basins demonstrate different degrees of spatial coherence in drought occurrence. The Nura–Sarysu and Esil WMBs exhibit relatively high spatial consistency, with major drought episodes occurring simultaneously across several or most meteorological stations. In the Nura–Sarysu WMB, particularly widespread droughts were identified in 1951–1952, 1977, 1988, 2005, 2012, and 2022. In the Esil WMB, widespread negative SPI-3 anomalies occurred in 1944–1945, 1963, 1975, 1989, 1991, 1995, 1997–1998, 2010, 2012, and 2021–2022. These synchronous episodes indicate a pronounced regional climatic signal affecting moisture conditions over relatively large areas.

In contrast, the Tobyl–Torgai WMB exhibits greater spatial heterogeneity. Although major drought episodes were frequently observed simultaneously at several stations, their intensity differed considerably between locations. The most widespread episodes occurred in 1943–1945, 1955, 1967, 1974–1975, 1991, 1995, 1998, 2004–2005, 2007–2009, 2010, 2012, and 2021–2023, with particularly strong negative anomalies during 1943–1945 and 2023. The lower spatial coherence compared with the Nura–Sarysu and Esil WMBs suggests a greater contribution of local climatic conditions to short-term moisture variability.

The temporal structure of the SPI-3 series also differs among the three basins. In the Nura–Sarysu WMB, drought frequency and intensity become more pronounced from the late 1970s onward, with several widespread events occurring during the 2000s and early 2020s. In the Esil WMB, relatively moderate variability during the 1950s–1970s is followed by a greater occurrence of widespread drought episodes from the late 1980s onward, including pronounced events in 1991, 2010, 2012, and 2021–2022. The Tobyl–Torgai WMB maintains recurrent drought conditions throughout the observation period, but without the same degree of spatial synchronization observed in the Nura–Sarysu and Esil WMBs.

Analysis of temporal structural changes further indicates that the observed evolution of SPI-3 conditions is not uniform across the three WMBs. Statistically significant change points identified in individual meteorological time series indicate shifts in the temporal structure of short-term moisture variability rather than a uniform basin-wide transition. The proportion of time series containing statistically significant change points therefore characterizes the prevalence of structural shifts among the available records and should not be interpreted as a quantitative "level of non-stationarity". This formulation provides a more precise interpretation of the detected temporal changes and distinguishes the occurrence of statistically significant structural shifts from the broader concept of climatic non-stationarity.

Overall, the comparison demonstrates that the Nura–Sarysu and Esil WMBs are characterized by stronger spatial coherence of drought conditions, whereas the Tobyl–Torgai WMB shows greater spatial heterogeneity and stronger local contrasts. Despite these differences, all three basins exhibit recurrent short-term moisture deficits and significant interannual variability. The identified temporal structural changes and differences in spatial coherence emphasize that drought dynamics across northern and central Kazakhstan are shaped by the combined influence of regional atmospheric processes and basin-specific climatic conditions. These results support the use of spatially resolved drought assessment rather than assuming a uniform temporal response across individual water management basins.

3.5. Standardized Precipitation Evapotranspiration Index

Under conditions of contemporary climatic warming, the assessment of drought requires accounting not only for changes in atmospheric precipitation but also for the increase in atmospheric moisture demand driven by rising air temperatures. In this regard, the standardized precipitation evapotranspiration index is widely used for the diagnosis of drought conditions, as it allows for the consideration of the combined influence of precipitation and potential evapotranspiration on the formation of moisture deficits.

The index is based on the water balance and provides a quantitatively comparable assessment of drought intensity, duration, and frequency across various time scales in both time and space. The application of this index enables the identification of the temperature-driven intensification of territorial aridity.

The SPEI-3 time series demonstrate pronounced interannual and multidecadal variability in hydrothermal conditions across the Nura–Sarysu, Esil, and Tobyl–Torgai WMBs, with recurrent alternation between dry and wet phases of different duration and intensity (Figures 4 and S4–S6). Compared with SPI-3, SPEI-3 additionally accounts for the influence of atmospheric evaporative demand and therefore reflects moisture deficits associated with both precipitation variability and temperature-dependent evapotranspiration.

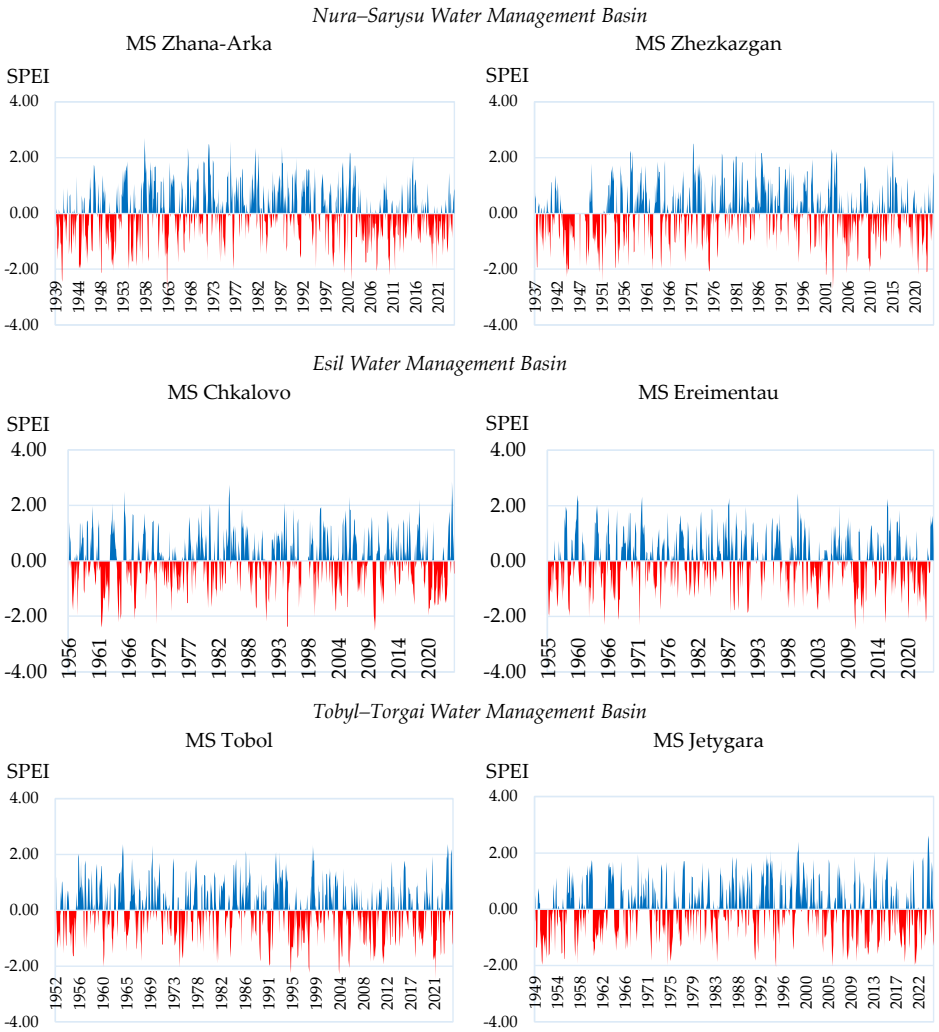

Figure 4. Long-term dynamics of the standardized precipitation evapotranspiration index SPEI-3 at the main meteorological stations of the study area.

In the Nura–Sarysu WMB, the most significant drought periods occurred in 1944–1946, 1963, 1974–1975, 1977, 1995, 2001–2002, 2005–2006, 2008–2010, and 2022–2023. The most severe and spatially coherent events were identified in 1963, 1977, 2001–2002, 2010, and 2022–2023, when negative SPEI-3 anomalies affected most meteorological stations and frequently reached severe to extreme drought thresholds (SPEI ≤ -1.5 and SPEI ≤ -2.0). The 1963 event was among the strongest droughts in the observation period, with an extreme SPEI minimum of -3.28 recorded at Zhana–Arka. The droughts of 2001–2002 and 2022–2023 were also characterized by extensive spatial coverage and extreme moisture deficits at several stations. The strongest negative SPEI-3 anomalies were frequently

observed at Zhana-Arka, Zhezkazgan, and Aksu–Ayuly, indicating pronounced spatial differences in the severity of hydrothermal moisture deficits within the basin.

In the Esil WMB, SPEI-3 also indicates pronounced interannual and multidecadal variability, with prolonged dry phases alternating with periods of increased moisture availability. The most significant drought periods occurred in 1939–1940, 1943–1945, 1951–1952, 1962, 1965–1967, 1974–1975, 1991, 1995, 1997, 2000, 2003, 2005–2006, 2010, and 2020–2022. Widespread wet phases were identified in 1946, 1964, 1969, 1977–1978, 1984, 1992–1994, 2001–2002, 2013–2017, and 2023–2024. The most spatially coherent drought events occurred in 1951–1952, 1991, 2010, and 2020–2022, affecting approximately 80–90% of meteorological stations. The 2010 event was particularly pronounced, with SPEI values below −2.0 recorded at most stations. The 2020–2022 period represents another extensive recent drought phase, characterized by persistent negative SPEI-3 values across a large part of the basin. The strongest negative extremes were frequently observed at Chkalovo, Saumalkol, Sergeyevka, and Vozvyshenka.

The Tobyl–Torgai WMB exhibits a similarly pronounced alternation of dry and wet phases but with greater spatial heterogeneity in the magnitude of SPEI-3 anomalies. Major drought episodes were frequently synchronous across several stations, indicating the influence of regional-scale hydroclimatic processes, while their intensity varied considerably between locations. The most significant drought periods occurred in the late 1930s–early 1940s, 1951–1952, the early 1960s, 1974–1975, the 1990s, 2005–2006, 2010, 2012, and 2020–2022. Wetter conditions were observed during the early 1960s, early 1970s, 1984, 1992–1994, 2001–2002, 2013–2016, and 2023–2024. The most spatially consistent drought episodes occurred in 1951–1952, 1995, 2010, and 2020–2022. The 2010 drought was among the strongest contemporary events, with severe to extreme moisture deficits (SPEI ≤ -2.0) recorded at several stations. The period 2020–2022 represents the longest recent drought phase, with persistent negative SPEI-3 values across most of the basin. The deepest negative extremes were most frequently recorded at Kushmurun, Tobol, Torgai, and Zhitykara.

A comparison of the three WMBs indicates stronger spatial coherence of SPEI-3 drought conditions in the Nura–Sarysu and Esil basins, whereas the Tobyl–Torgai WMB demonstrates greater spatial heterogeneity. Several major drought episodes, particularly those in 1951–1952, 1974–1975, 1995, 2010, and 2020–2022, occurred contemporaneously in more than one basin, indicating the presence of regional-scale hydroclimatic forcing. At the same time, differences in drought intensity among individual stations demonstrate the importance of local climatic conditions and spatial variability in temperature and precipitation.

The temporal structure of SPEI-3 also shows periods of statistically detectable structural change in individual station series. These change points indicate shifts in the statistical characteristics of hydrothermal moisture variability at particular locations rather than a uniform transition across an entire WMB. Accordingly, the proportion of station series containing statistically significant change points can be interpreted as the spatial prevalence of temporal structural shifts within each basin. This measure provides a direct characterization of how widespread statistically detectable changes are among the available records.

Overall, the SPEI-3 analysis demonstrates recurrent and spatially heterogeneous drought conditions across all three WMBs. The Nura–Sarysu and Esil basins show relatively high spatial coherence in major drought events, while Tobyl–Torgai is characterized by stronger local contrasts. The repeated occurrence of severe and extreme SPEI-3 anomalies in recent decades, including the widespread events of 2010 and 2020–2022/2023, highlights the importance of considering both precipitation variability and temperature-related atmospheric evaporative demand when assessing drought development in northern and central Kazakhstan. The identified structural shifts and spatial differences further support the use

of station-level and spatially resolved drought assessment rather than assuming a uniform hydroclimatic response within individual water management basins.

3.6. Quantitative Assessment of the Spatial Coherence of Meteorological Droughts

To quantitatively assess the spatial consistency of major meteorological drought episodes, we calculated the maximum proportion of weather stations that simultaneously exhibited SPI-3 or SPEI-3 ≤ -1.0 (Table 9). The calculation was performed relative to the actual number of stations with available observations for the corresponding time step, which allowed for the varying lengths of the observation series.

Table 9. Maximum spatial coherence of major meteorological drought episodes in the studied river basins.

WMB	Period	SPI-3, Max SC, %	n/N	SPEI-3, Max SC, %	n/N
Nura–Sarysu	1951–1952	100	5/5	100	6/6
	1977	85.7	6/7	100	8/8
	1988	100	7/7	75	6/8
	2001–2002	85.7	6/7	100	8/8
	2005–2006	85.7	6/7	100	8/8
	2010	85.7	6/7	87.5	7/8
	2012	85.7	6/7	75	6/8
	2022–2023	85.7	6/7	100	8/8
Esil	1944–1945	100	10/10	100	10/10
	1991	94.4	17/18	93.8	15/16
	1995	93.8	15/16	93.8	15/16
	1997–1998	82.4	14/17	94.4	17/18
	2010	94.4	17/18	94.4	17/18
	2012	83.3	15/18	83.3	15/18
	2021–2022	66.7	12/18	88.9	16/18
Tobyl–Torgay	1943–1945	100	5/5	100	5/5
	1955	85.7	6/7	100	7/7
	1974–1975	90.0	9/10	100	9/9
	1991	88.9	8/9	100	8/8
	1995	88.9	8/9	100	9/9
	1998	66.7	6/9	100	10/10
	2004–2005	80.0	8/10	100	10/10
	2010	66.7	6/9	100	9/9
	2012	90.0	9/10	100	10/10
	2021–2023	87.5	7/8	100	8/8

Note: n—the number of stations that simultaneously met the criterion SPI-3/SPEI-3 ≤ -1.0; N—the number of stations for which data were available in the corresponding time step; SC—spatial coherence.

The results confirmed a strong spatial consistency among most major drought episodes, but revealed significant differences between SPI-3 and SPEI-3. In the Esil water management basin, the maximum spatial coverage in 1991 and 2010 exceeded 93% for both indices. During the 2021–2022 period, the differences between the indices were more pronounced-the maximum proportion of affected stations was 66.7% for SPI-3 and 88.9% for SPEI-3.

When interpreting the obtained values, one should take into account differences in the climatic periods used to standardize individual station time series. Therefore, the reported spatial coherence indicators primarily characterize the synchrony of stations' transition into the category of moderate and more severe drought (SPI-3/SPEI-3 ≤ -1.0), rather than the absolute identity of the standardized index values between stations.

In the Nura–Sarysu WMB, severe droughts were also characterized by high spatial consistency, with maximum values ranging from 85.7 to 100% for most of the episodes under consideration. In the Tobyl–Torgay WMB, the spatial extent based on SPI-3 was more variable, ranging from 66.7 to 100%, whereas for SPEI-3, a number of major episodes showed synchronous drought at all stations with observations during the corresponding period. The results show that the most significant drought episodes were characterized by

pronounced spatial consistency, although their magnitude depended on both the specific event and the index used.

The additional presentation of the SPI-3 and SPEI-3 time series in a "station × time" format on a unified time axis spanning 1930–2024 confirms that the most severe drought episodes were characterized by the simultaneous occurrence of negative anomalies across a significant portion of the observation network (Figures 5 and 6). At the same time, the heat maps demonstrate varying network coverage during early observation periods, which confirms the need to calculate spatial consistency relative to the actual number of stations with available data at each time step.

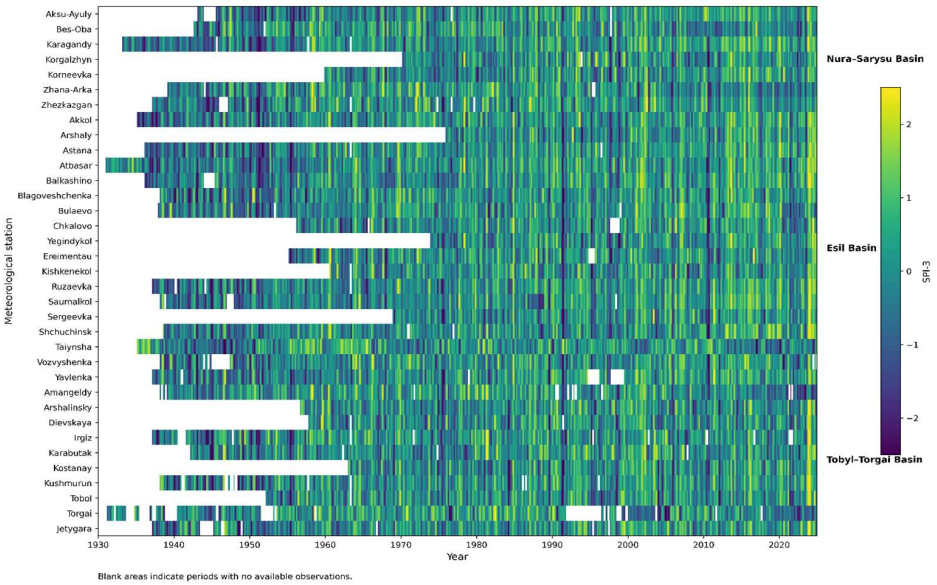

Figure 5. Spatiotemporal distribution of SPI-3 across weather stations in the Nura–Sarysu, Esil, and Tobyl–Torgay water management basins, 1930–2024. Blank areas correspond to periods for which no observations are available.

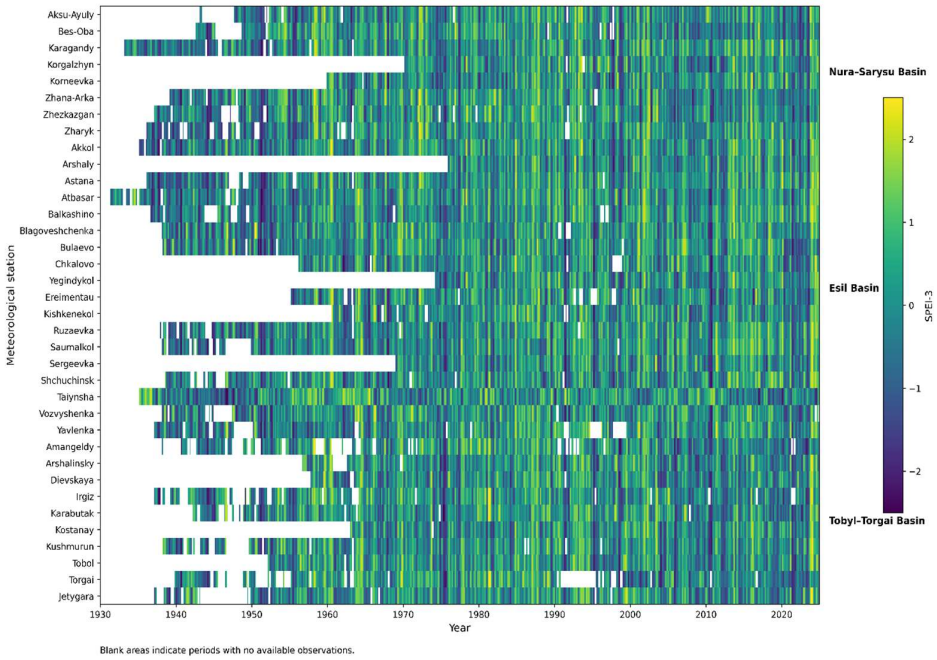

Figure 6. Spatiotemporal distribution of SPEI-3 across weather stations in the Nura–Sarysu, Esil, and Tobyl–Torgay water management basins, 1930–2024. Blank areas correspond to periods for which no observations are available.

3.7. Streamflow Drought Index

The 12-month SDI analysis demonstrates pronounced interannual and multiannual variability in water availability across the Nura–Sarysu, Esil, and Tobyl–Torgai WMBs, with recurrent alternation between hydrological drought and wet phases of different duration and intensity (Figures 7 and S7–S9). Despite substantial differences in basin characteristics and runoff sensitivity, major hydrological anomalies were frequently observed synchronously across multiple gauging stations, indicating a strong regional component of runoff variability. At the same time, the spatial expression of individual drought and wet phases varied considerably among rivers, particularly between large rivers and smaller catchments.

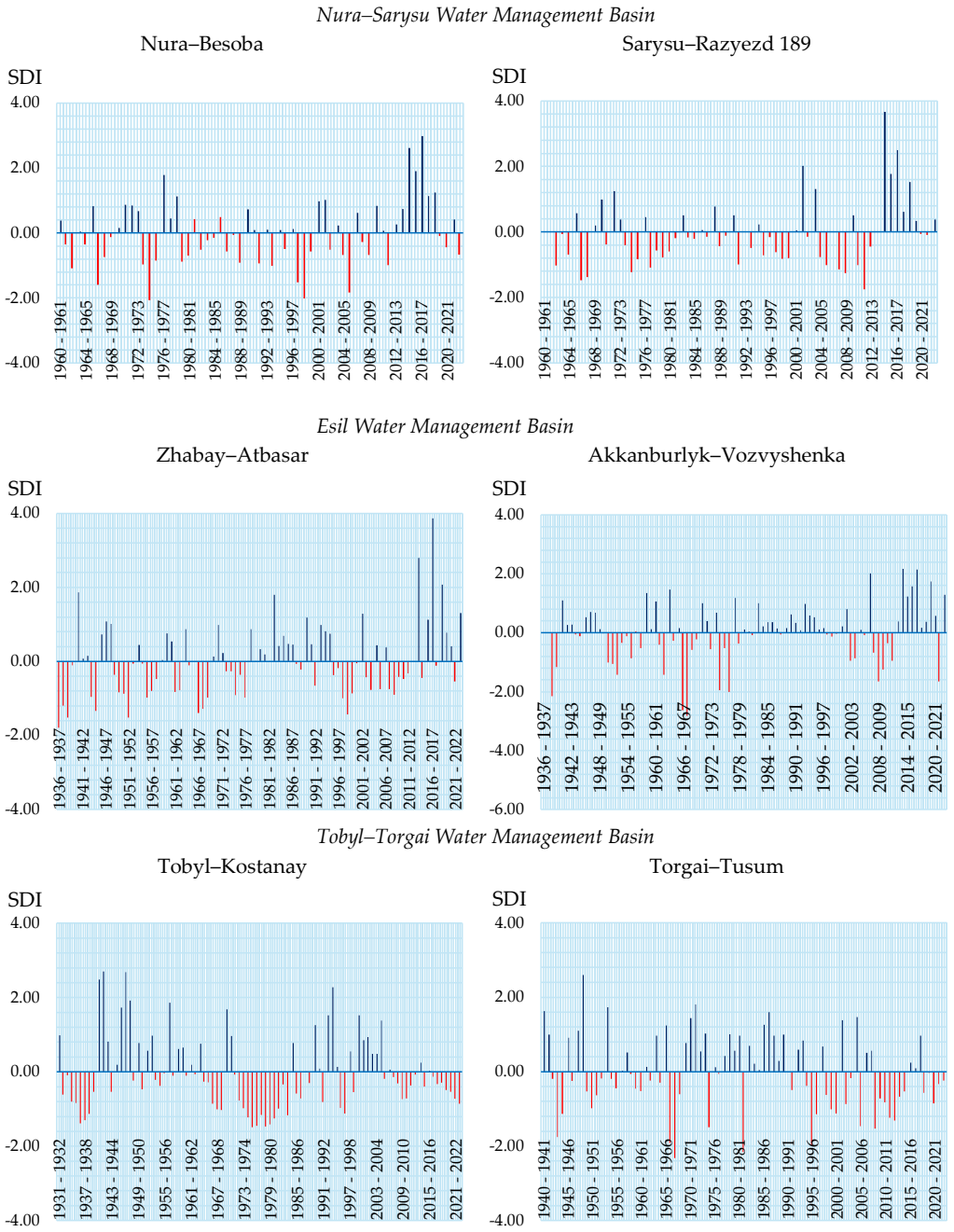

Figure 7. Long-term dynamics of the Streamflow Drought Index SDI-12 at the main hydrological posts of the study area, based on a combination of observed and reconstructed data.

Across all three WMBs, hydrological droughts were generally more persistent than wet phases and, in many cases, affected a larger proportion of the gauging network. The most pronounced drought conditions occurred during the mid-1960s, particularly in 1966–1969, when severe runoff deficits were recorded simultaneously across the Esil and Tobyl–Torgai WMBs and substantial negative SDI anomalies were also observed in the Nura–Sarysu WMB. Other widespread drought phases were identified in the 1970s, especially 1974–1977, as well as during the late 1990s and early 2000s. The recurrence of these periods across geographically distinct basins indicates that large-scale climatic variability exerted a substantial influence on the regional hydrological regime.

The late twentieth and early twenty-first centuries were characterized by another sequence of pronounced hydrological anomalies. In the Nura–Sarysu WMB, major drought phases occurred in 1997–2001 and 2005–2009, whereas the Esil and Tobyl–Torgai WMBs exhibited particularly persistent runoff deficits during 1997–2001 and 2008–2009. The Tobyl–Torgai WMB additionally experienced a prolonged drought during 1991–1997, demonstrating that the duration and intensity of hydrological deficits may differ substantially even when anomalies occur within the same broader climatic period. In the most recent period, moderately dry conditions were evident in parts of the Nura–Sarysu WMB during 2018–2023 and in the Tobyl–Torgai WMB during 2018–2022, suggesting a continuation of recurrent runoff-deficit conditions in some areas.

Wet phases were generally shorter and more episodic than droughts, although several periods demonstrated strong spatial synchronization. The most consistent periods of increased water availability occurred during 1989–1994 and 2013–2017. The 1989–1994 wet phase was particularly pronounced in the Nura–Sarysu and Tobyl–Torgai WMBs, while 2013–2017 represented the strongest wet period in the Esil WMB and one of the most pronounced periods of increased water availability across the study region. The SDI values during these periods occasionally reached extreme positive values, exceeding +3.0 in the Nura–Sarysu WMB and reaching +3.9 on the Zhabay River in the Esil WMB. The occurrence of coherent wet phases across several basins further supports the importance of regional-scale climatic forcing in determining periods of anomalously high runoff.

The comparison of the three WMBs reveals distinct spatial characteristics of hydrological variability. The Nura–Sarysu basin demonstrates a high degree of synchronization of drought conditions, with the upper Nura River, particularly the Nura–Besoba and Nura–Balykty gauging stations, showing strong sensitivity to runoff deficits. In the Sarysu basin, drought anomalies tend to be weaker but more persistent. The Esil WMB is characterized by strong regional coherence of major hydrological extremes, while smaller rivers such as Kalkutan, Akkanburlyk, and Imanburlyk exhibit greater SDI variability than the main Esil River. This contrast can be associated with differences in catchment size and hydrological buffering capacity. A similar pattern is evident in the Tobyl–Torgai WMB, where smaller and medium-sized rivers, including Karatorgai, Uly Zhilanshyk, and Irgiz, demonstrate stronger SDI fluctuations and deeper negative anomalies than the larger Tobyl River.

A pronounced spatial gradient is also evident within the Tobyl–Torgai WMB. Southern and central parts of the basin tend to exhibit earlier and more intense drought anomalies, whereas northern rivers demonstrate a more gradual response and stronger positive SDI anomalies during wet periods. This spatial differentiation, together with the contrasting behavior of small and large catchments in the Esil and Nura–Sarysu WMBs, indicates that regional climatic forcing is modified by basin-scale characteristics that control the magnitude and persistence of runoff anomalies.

Taken together, the SDI results indicate that the three WMBs share a common sequence of major hydrological extremes, while their magnitude and duration remain spatially heterogeneous. The recurrent occurrence of synchronized drought and wet phases suggests

that regional climatic variability represents an important control on long-term runoff fluctuations. However, runoff formation conditions and hydrological regulation contribute to substantial variations in the sensitivity of individual rivers. Consequently, hydrological drought represents a more persistent and spatially coherent component of water availability variability than wet conditions, whereas extreme wet phases tend to be more episodic but can affect large portions of the region simultaneously.

The temporal evolution of SDI anomalies is also consistent with the presence of distinct periods of changing hydrological behavior identified through the analysis of statistically significant structural shifts (change points). Identified changes represent statistically significant modifications in the structure of individual time series and do not imply a uniform or continuous transition in the hydrological regime across the three basins. The combination of SDI dynamics and identified structural shifts therefore provides complementary evidence of substantial temporal variability in water availability while preserving the spatial heterogeneity of hydrological responses among the Nura–Sarysu, Esil, and Tobyl–Torgai WMBs.

A comparison of the temporal dynamics of meteorological and hydrological indices revealed differences in the duration and temporal persistence of the identified drought conditions. The short-term SPI-3 and SPEI-3 were characterized by more pronounced monthly variability, whereas the SDI-12 reflected longer-lasting and time-smoothed hydrological conditions. This difference is consistent with the integral nature of the SDI-12, which is based on the accumulated volume of river flow over a longer time interval. However, given the difference in the time scales of the indices used, the observed shift in SDI-12 minima relative to individual SPI-3/SPEI-3 episodes was not interpreted as a quantitatively established delay in drought propagation.

The relationship of hydrological drought characteristics with the catchment area. To quantify the possible effect of watershed size on the severity of hydrological drought, a correlation analysis was performed for 29 hydrological posts (Table 10).

Table 10. Relation of the catchment area to the SDI-12 characteristics for the studied hydrological posts.

Characteristic of SDI-12	Spearman ρ	*p*-Value	Statistical Significance
Standard deviation of SDI-12	0.164	0.397	Not significant
Minimum SDI-12	0.100	0.606	Not significant
Drought frequency (SDI-12 ≤ -1.0), %	0.238	0.214	Not significant

Note: For catchments with drainless areas, the effective catchment area was used; statistical significance was estimated at $p < 0.05$.

Quantitative analysis did not reveal a statistically significant monotonic relationship between catchment area and the SDI-12 characteristics under consideration. For the standard deviation of SDI-12, ρ = 0.164 (p = 0.397) was obtained; for the minimum SDI-12 value, ρ = 0.100 (p = 0.606); and for the frequency of hydrological drought, ρ = 0.238 (p = 0.214). Thus, none of the tested relationships was statistically significant at a significance level of $p < 0.05$.

The results obtained do not confirm the existence of a general monotonic relationship between the catchment area size and variability, minimum values, or frequency of hydrological drought in the sample under study.

4. Discussion

The results demonstrate substantial spatiotemporal variability in meteorological and hydrological drought conditions across northern and central Kazakhstan. The combined analysis of SPI, SPEI, and SDI shows that drought characteristics differ among the Nura–Sarysu, Esil, and Tobyl–Torgai WMBs, reflecting the combined influence of precipitation variability, atmospheric water demand, and basin-specific runoff-generation processes. Such interactions

are particularly important in semi-arid continental regions, where relatively small changes in temperature and precipitation can substantially affect water availability.

The identified structural shifts in meteorological and hydrological drought indices indicate significant changes in the statistical characteristics of the analyzed time series during the instrumental period. The main concentrations of change points, including the mid-twentieth century, 1965–1977, the late 1990s, and the early 2000s, coincide with periods of pronounced hydroclimatic variability reported in previous studies. These findings are consistent with research documenting changes in climatic variability, atmospheric circulation, and drought characteristics across Kazakhstan and Central Asia [14,16,31,32]. Recent studies have also shown that global warming can intensify hydroclimatic contrasts and increase drought duration and severity in arid and semi-arid regions [11,15]. Similar tendencies have been reported across Central Asia, where increasing aridization and more persistent drought conditions have become particularly evident during recent decades [33]. The present results are broadly consistent with these regional findings, while also demonstrating substantial spatial differentiation among the three water management basins.

A notable result is the different behavior of SPI and SPEI. A higher frequency of detected structural shifts in SPI than in SPEI should not be interpreted as direct evidence that precipitation is the dominant driver of abrupt changes in drought characteristics. SPI is based exclusively on precipitation, whereas SPEI incorporates precipitation and potential evapotranspiration and therefore represents a standardized climatic water-balance signal. Differences between the two indices may consequently reflect the combined and potentially compensating effects of precipitation and atmospheric evaporative demand. Similar mechanisms, whereby increasing atmospheric water demand can intensify drought conditions even in the absence of a substantial decline in precipitation, have been reported in previous studies [28,32,34,35]. The use of the FAO-56 Penman–Monteith method provides a physically based estimate of potential evapotranspiration; nevertheless, SPEI remains a climatic water-balance indicator and does not directly represent the complete hydrological response of river systems.

The comparison of the three WMBs reveals distinct spatial patterns of drought variability. The Esil WMB demonstrates the highest spatial coherence of major drought events, indicating a relatively strong regional component in the atmospheric forcing of drought conditions. In contrast, the Tobyl–Torgai WMB exhibits greater spatial heterogeneity, which may reflect stronger climatic gradients, differences in basin morphology, and variations in runoff-generation mechanisms. The Nura–Sarysu WMB occupies an intermediate position, combining pronounced regional coherence during major drought episodes with differences among individual sub-basins. These spatial patterns are consistent with previous assessments of Central Asian hydroclimatic variability, which emphasize the roles of atmospheric circulation, continentality, and regional environmental characteristics in determining spatial differences in climate response [17,36,37].

The hydrological drought analysis further demonstrates that the direction and magnitude of SDI changes vary among basins. Positive shifts in the mean SDI are prevalent in the Nura–Sarysu and Esil WMBs, whereas the Tobyl–Torgai WMB contains both positive and negative changes. These differences indicate that changes in observed river-flow characteristics are spatially heterogeneous and depend on the specific conditions of water-resource formation in individual basins. Because SDI is derived from observed streamflow, its structural changes represent the integrated response of river systems to climatic variability and basin-specific hydrological and water-management processes. Therefore, the spatial differences in SDI cannot be interpreted solely in terms of atmospheric drought conditions.

The initial assumption that smaller watersheds are characterized by a more pronounced response to hydrological drought was not quantitatively confirmed. For the

29 hydrological stations studied, no statistically significant monotonic relationship was found between catchment area and the standard deviation of the SDI-12, its minimum value, or the frequency of SDI-12 ≤ -1.0 conditions. Consequently, the observed differences in hydrological drought among rivers cannot be explained by catchment size alone.

The results indicate a more complex nature of hydrological drought formation in the studied basins. Catchment size may determine part of a river system's storage capacity and inertia; however, the actual response of runoff is shaped by the combined effects of the spatial distribution of precipitation and snowpack, snowmelt patterns, groundwater recharge, water losses and accumulation within the basin, as well as river flow regulation and water use. Therefore, the influence of catchment area should be considered in conjunction with other physical-geographical and water management characteristics, rather than as a standalone explanation for differences in SDI-12.

The longer and smoother temporal behavior of SDI-12 compared with SPI-3 and SPEI-3 reflects the different timescales represented by the indices. SPI-3 and SPEI-3 characterize relatively short-term meteorological and climatic water-balance anomalies, whereas SDI-12 integrates variations in river flow over a substantially longer period. Consequently, hydrological drought characteristics are generally more persistent and less sensitive to individual short-term precipitation anomalies. The difference in temporal behavior is consistent with the established distinction between meteorological and hydrological drought development and with the use of multi-timescale indices in drought propagation studies [38,39]. In the present study, however, this difference in timescale is interpreted as a distinction in temporal persistence rather than as a quantitative estimate of drought propagation time.

The results also have implications for the interpretation of long-term drought variability. The occurrence of alternating periods of pronounced drought and wet conditions demonstrates that drought characteristics vary considerably over the instrumental record. Periods of positive and negative SDI anomalies are observed across all three WMBs, but their duration, magnitude, and spatial coherence differ among basins. The recurrence of major drought and wet phases across several independent time series suggests a regional component of hydroclimatic variability, while the differences in their local expression highlight the importance of basin-specific processes.

The structural shifts identified by the change-point analysis provide an additional perspective on these long-term variations. Their temporal clustering indicates that the statistical characteristics of several drought-index series changed during particular periods. When changes occur with temporal consistency across several independent meteorological or hydrological series and coincide with corresponding changes in climatic characteristics, they may indicate a regional association with broader hydroclimatic variability. However, individual change points should not be interpreted as direct evidence of a specific physical cause or as definitive evidence of a transition to a new hydroclimatic regime. This distinction is particularly important for long instrumental records, in which statistical changes may also be affected by observation-network characteristics and other sources of uncertainty, as discussed in the Study Limitations section.

From an applied perspective, the combined use of SPI, SPEI, and SDI provides a complementary framework for drought monitoring. SPI characterizes precipitation deficits, SPEI additionally incorporates atmospheric evaporative demand, and SDI describes the resulting variability in observed river flow. Their joint interpretation makes it possible to distinguish atmospheric drought conditions from changes in hydrological water availability and to identify periods when drought signals are spatially coherent across several components of the water system. Such an integrated approach is particularly relevant for northern and central Kazakhstan, where water resources support agricultural production, industry, urban systems, and ecosystems.

Overall, the results demonstrate that drought variability across the Nura–Sarysu, Esil, and Tobyl–Torgai WMBs is characterized by pronounced temporal variability and substantial spatial differentiation. The spatial coherence of major drought episodes points to a regional climatic component, whereas differences in SDI characteristics reflect the influence of basin-specific runoff formation, storage, and water-management conditions. The combined interpretation of SPI, SPEI, and SDI therefore provides a more comprehensive basis for assessing drought variability and for supporting water-resource planning under changing climatic conditions.

Study Limitations

Several limitations should be considered when interpreting the results of the present study.

First, the duration of the observation records varies because meteorological and hydrological observations in the study area began in different years. Consequently, the number of stations and hydrological gauges available for comparison changes over time. To reduce the associated bias, spatial consistency was assessed relative to the actual number of active stations for which observations were available during the corresponding period, rather than relative to a fixed total number of stations. Nevertheless, the earliest periods are represented by a smaller number of observation points and therefore have greater spatial uncertainty.

Second, the density of the observation network differs among the Nura–Sarysu, Esil, and Tobyl–Torgai WMBs. The calculated characteristics of spatial consistency should therefore be interpreted as the degree of consistency within the available observation network rather than as uniform spatial representation of the entire area of each basin. This limitation is particularly relevant when comparing basins that differ in the number and spatial distribution of meteorological stations.

Third, some river-flow time series required the reconstruction of individual missing values. Although reconstruction improves the temporal continuity of the series and enables long-term analysis, reconstructed values cannot be considered fully equivalent to direct instrumental observations. They therefore introduce additional uncertainty into SDI estimates and structural change detection. In the verified series, no statistically significant breakpoints directly coincided with reconstructed years; however, for some stations, a detected breakpoint occurred within one year of a reconstructed value. In such cases, the possible influence of the reconstruction procedure on the local structure of the time series cannot be completely excluded. These change points were therefore interpreted with caution and were not considered independently as evidence of a physical change in the hydrological regime.

Fourth, river flow in the studied WMBs is affected not only by climate variability but also by flow regulation, water abstraction, redistribution of water resources, and other anthropogenic factors. Consequently, SDI represents an integrated response of the hydrological system to both natural and water-management influences. The present study does not provide a quantitative separation of these components. In the Esil WMB, for example, significant flow regulation is associated with the Vyacheslavskoye and Sergeyevskoye reservoirs; the Tobyl–Torgai WMB also contains major regulatory reservoirs, while the Nura–Sarysu WMB includes a system of reservoirs, including the Samarkand Reservoir. Therefore, temporal coincidence between an SDI change point and a period of climatic change cannot by itself be considered sufficient evidence of climatic attribution. Formal attribution would require additional information on water abstraction, reservoir operating regimes, irretrievable water consumption, and other water-management factors.

Fifth, uncertainty is associated with the calculation of potential evapotranspiration used to derive SPEI. Uncertainties in the input meteorological observations and in the PET estimation procedure are propagated into the climatic water-balance calculation and,

consequently, into SPEI values. Therefore, differences between SPI and SPEI should be interpreted as differences between a precipitation-only signal and an integrated climatic water-balance signal; they do not permit the independent quantitative contribution of temperature or atmospheric evaporative demand to be determined.

Sixth, the detection of a statistically significant change point should be interpreted as evidence of a change in the statistical properties of the analyzed time series rather than as unambiguous evidence of a specific physical transition of the hydroclimatic system to a new regime. Change-point detection can be affected by the length of the time series, serial dependence, individual extreme events, and anthropogenic influences. The physical interpretation of individual change points is therefore necessarily cautious. In addition, statistical heterogeneity in long instrumental records may potentially result from changes in the observation network, including station relocation, replacement of instruments, changes in observation procedures, or changes in local measurement conditions. Complete historical metadata documenting such changes were not available for all observation sites throughout the entire study period. Consequently, individual change points identified by the Pettitt, Buishand, SNHT, and CUSUM tests were interpreted primarily as statistical structural shifts. Greater confidence was placed in changes consistently identified by several statistical tests and manifested across several independent time series. The additional assessment of serial correlation and multiple-testing correction using the false discovery rate method further supports cautious interpretation of individual significance results.

Seventh, the different lengths of the meteorological time series result in differences in the periods used to standardize SPI and SPEI. Because standardized indices are calculated relative to the statistical characteristics of the selected reference period, differences in its duration and temporal coverage can affect the absolute index values, particularly in the presence of long-term changes in temperature and precipitation. Accordingly, inter-station comparison in the present study focuses primarily on the temporal synchrony of categorical drought conditions and the spatial extent of events, while differences in absolute SPI and SPEI values are interpreted with caution.

Finally, the present study was designed to identify spatiotemporal patterns, consistency, and structural changes in meteorological and hydrological droughts rather than to quantitatively attribute changes in river flow to individual causal factors or estimate a formal drought-propagation lag. SPI-3, SPEI-3, and SDI-12 characterize processes at different temporal scales; therefore, their temporal differences cannot be directly converted into a quantitative propagation time. Such an assessment would require comparable continuous monthly meteorological and hydrological series and dedicated methods such as lagged cross-correlation or other drought-propagation approaches [38,40]. Similarly, separating the contributions of climatic forcing, reservoir regulation, water abstraction, land-use changes, and other anthropogenic factors would require additional water-management data and specialized attribution methods. The results should therefore be regarded as evidence of observed changes in the statistical characteristics and spatiotemporal consistency of hydroclimatic time series, rather than as a quantitative assessment of the contribution of individual factors to changes in the hydrological regime.

5. Conclusions

This study investigated the long-term evolution of meteorological and hydrological droughts in the Nura–Sarysu, Esil, and Tobyl–Torgai WMBs of northern and central Kazakhstan using SPI, SPEI, SDI, and homogeneity tests. The main findings are as follows:

1. The long-term dynamics of droughts in the study basins are characterized by pronounced non-stationarity; however, the magnitude and temporal localization of structural changes differ substantially among the basins and the indices used. For

SPI-3, statistically significant structural shifts were identified at 88% of meteorological stations in the Nura–Sarysu WMB, 72% in the Esil WMB, and 55% in the Tobyl–Torgai WMB, whereas for SPEI-3, the corresponding values were 62%, 56%, and 27%. Across the entire study network, the proportion of time series with significant structural changes was 70% for SPI-3 and 49% for SPEI-3. The most pronounced periods of restructuring in meteorological drought characteristics occurred in the mid-twentieth century (1965–1977) and the late twentieth to early twenty-first century. The results indicate that assuming stationarity across the entire observation period may inadequately represent the long-term variability of drought conditions.

2. Pronounced spatial heterogeneity of droughts was identified among the three WMBs. The highest spatial consistency of meteorological droughts was characteristic of the Esil WMB, where the major episodes of 1951–1952, 1991, 2010, and 2020–2022 affected approximately 80-90% of active meteorological stations. The Tobyl–Torgai WMB was characterized by greater spatial heterogeneity, whereas the Nura–Sarysu WMB occupied an intermediate position. Therefore, major droughts across the study area occur as regionally coherent events; however, the degree of their spatial synchrony depends on the specific basin and the structure of the available observation network. The high spatial consistency of the Esil WMB and the coverage of 80–90% of stations are directly presented in the results of the article.
3. Comparison of SPI-3 and SPEI-3 revealed different patterns of changes in atmospheric moisture and the climatic water balance signals. The higher proportion of structural shifts in SPI-3 compared with SPEI-3 indicates a more pronounced sensitivity of the precipitation signal to abrupt changes, whereas the inclusion of potential evapotranspiration in SPEI produces a smoother pattern of long-term changes. In recent decades, the differences between SPI and SPEI have become particularly important for interpreting changes in drought under observed warming. However, these differences should not be considered a quantitative assessment of the independent contribution of temperature or atmospheric evaporative demand without a dedicated attribution analysis.
4. The analysis of SDI-12 showed that hydrological droughts have their own spatiotemporal structure and are not always synchronized with meteorological droughts. River flow is characterized by smoother and prolonged periods of water deficit, while the timing of detected structural changes in SDI differs from those in SPI and SPEI. The most notable stages of restructuring of the hydrological time series occurred in 1976–1981, 1988–1993, and 2009–2012. At the same time, the direction of changes was not uniform. In the Nura–Sarysu and Esil WMBs, positive changes in mean SDI predominated at a number of gauges, whereas both positive and negative changes were identified in the Tobyl–Torgai WMB. This confirms the need to account separately for the hydrological response when assessing droughts, rather than directly equating it with the meteorological signal.

   An additional quantitative analysis for 29 hydrological stations did not reveal a statistically significant monotonic relationship between catchment area and SDI-12 variability, the minimum index value, or the frequency of hydrological drought. Consequently, differences in hydrological response among the studied rivers cannot be explained solely by catchment size and require consideration of a combination of natural and water management factors influencing runoff formation.
5. The combined use of SPI, SPEI, and SDI makes it possible to characterize different components of drought development, such as precipitation deficits, changes in the climatic water balance, and actual variability in river flow. At the same time, SDI reflects the integrated response of the river system not only to climatic conditions

but also to runoff-generation and flow-regulation processes and other anthropogenic impacts. Therefore, the identified temporal and spatial consistency between meteorological and hydrological indices indicates the interconnectedness of the observed hydroclimatic changes but, by itself, does not constitute evidence that changes in river flow are caused exclusively by climatic factors. In the study water management basins, the hydrological response is shaped by the combined effects of climate variability, runoff-generation processes, reservoir regulation, and water use.

6. The results obtained have practical implications for drought monitoring and water resources management in Northern and Central Kazakhstan. The identified differences in spatial consistency, the timing of structural changes, and the response of hydrological time series demonstrate the need to move from unified stationary drought characteristics to a basin-oriented monitoring system that accounts for the non-stationarity of climatic and hydrological time series. The combined analysis of SPI, SPEI, and SDI can serve as a basis for identifying developing drought conditions and providing information support for early warning systems and adaptive water resources management.

Supplementary Materials: The following are available online at https://www.mdpi.com/article/10.3390/environments13100520/s1, Figure S1. Long-term dynamics of the standardized precipitation index SPI-3 at the main meteorological stations of the Nura-Sarysu water management basin. Figure S2. Long-term dynamics of the standardized precipitation index SPI-3 at the main meteorological stations of the Esil water management basin. Figure S3. Long-term dynamics of the standardized precipitation index SPI-3 at the main meteorological stations of the Tobyl–Torgai water management basin. Figure S4. Long-term dynamics of the standardized precipitation evapotranspiration index SPEI-3 at the main meteorological stations of the Nura-Sarysu water management basin. Figure S5. Long-term dynamics of the standardized precipitation evapotranspiration index SPEI-3 at the main meteorological stations of the Esil water management basin. Figure S6. Long-term dynamics of the standardized precipitation evapotranspiration index SPEI-3 at the main meteorological stations of the Tobyl–Torgai water management basin. Figure S7. Long-term dynamics of the Streamflow Drought Index SDI-12 at the main hydrological posts of the Nura-Sarysu water management basin, based on a combination of observed and reconstructed data. Figure S8. Long-term dynamics of the Streamflow Drought Index SDI-12 at the main hydrological posts of the Esil water management basin, based on a combination of observed and reconstructed data. Figure S9. Long-term dynamics of the Streamflow Drought Index SDI-12 at the main hydrological posts of the Tobyl–Torgai water management basin, based on a combination of observed and reconstructed data. Table S1. Results of the Mann–Kendall test and Sen's slope estimator for seasonal and annual air temperature time series. Table S2. Change points in long-term air temperature time series identified using the Pettitt test. Table S3. Results of the Mann–Kendall test and Sen's slope estimator for seasonal and annual pre-cipitation time series. Table S4. Change points in seasonal and annual precipitation time series identified using the Pettitt test. Table S5. Results of time-series homogeneity tests for SPI-3-month. Table S6. Results of time-series homogeneity tests for SPEI-3-month. Table S7. Characteristics of Identified Structural Changes in the Hydrological Regime Based on Statistical Test Results.

Author Contributions: Conceptualization, L.M. and H.V.; methodology, L.M. and H.V.; software, M.D. and A.K.; validation, M.D., G.K. and L.B.; formal analysis, M.D., E.T. and L.B.; investigation, M.D., A.D., M.Z. and E.T.; resources, H.V.; data curation, M.D., A.K. and G.K.; writing—original draft preparation, M.D., G.K., A.D., M.Z., A.K. and M.-E.R.-C.; writing—review and editing, L.M., M.-E.R.-C. and J.R.-I.; visualization, M.-E.R.-C. and J.R.-I.; supervision, L.M., M.-E.R.-C. and J.R.-I.; project administration, L.M. and E.T. All authors have read and agreed to the published version of the manuscript.

Funding: This research was funded by the Science Committee of the Ministry of Science and Higher Education of the Republic of Kazakhstan, Grant No. AP25794529, within the project "Development of adaptive water management systems in the Yesil River basin".

Data Availability Statement: The data presented in this study may be obtained on request from the corresponding authors.

Conflicts of Interest: The authors declare no conflicts of interest.

References

1. United Nations Office for Disaster Risk Reduction. *GAR 2021 Special Report on Drought: Summary for Policymakers*; UNDRR: Geneva, Switzerland, 2021. Available online: https://www.undrr.org/media/72527/download?startDownload=true (accessed on 2 March 2026).
2. Gringof, I.G. Zasukhi i opustynivanie—Ekologicheskie problemy sovremennosti. *Tr. VNIISKhM* **2000**, *33*, 14–40.
3. Zolotokrylin, A.N. *Klimaticheskoe Opustynivanie*; Nauka: Moscow, Russia, 2003; 245p.
4. Birimbayeva, L.; Makhmudova, L.; Alimkulov, S.; Tursunova, A.; Mussina, A.; Tigkas, D.; Beksultanova, Z.; Rodrigo-Clavero, M.-E.; Rodrigo-Ilarri, J. Analysis of the spatiotemporal variability of hydrological drought regimes in the lowland rivers of Kazakhstan. *Water* **2024**, *16*, 2316. [CrossRef]
5. Alimkulov, S.; Makhmudova, L.; Talipova, E.K.; Baspakova, G.; Tigkas, D.; Gulsaira, I. Response of the water level of the Balkash Lake to the distribution of meteorological and hydrological droughts under the conditions of climate change. *J. Water Clim. Change* **2024**, *15*, 3395–3408. [CrossRef]
6. Alimkulov, S.; Makhmudova, L.; Talipova, E.; Baspakova, G.; Monkayeva, G. Assessment of the impacts of climate change on drought intensity and frequency using SPI and SPEI in the Southern Pre-Balkash region, Kazakhstan. *Watershed Ecol. Environ.* **2025**, *7*, 11–22. [CrossRef]
7. Wong, G.; Van Lanen, H.A.J.; Torfs, P.J.J.F. Probabilistic analysis of hydrological drought characteristics using meteorological drought. *Hydrol. Sci. J.* **2013**, *58*, 253–270. [CrossRef]
8. Jiang, H.; Khan, M.A.; Li, Z.; Ali, Z.; Ali, F.; Gul, S. Regional drought assessment using improved precipitation records under auxiliary information. *Tellus A Dyn. Meteorol. Oceanogr.* **2020**, *72*, 1–26. [CrossRef]
9. Yerdelen, C.; Abdelkader, M.; Eris, E. Assessment of drought in SPI series using continuous wavelet analysis for Gediz Basin, Turkey. *Atmos. Res.* **2021**, *260*, 105687. [CrossRef]
10. Wilhite, D.A. Drought as a natural hazard: Concepts and definitions. In *Droughts: Global Assessment*; Wilhite, D.A., Ed.; Routledge: London, UK, 2000; pp. 3–18.
11. Dai, A. Drought under global warming: A review. *Wiley Interdiscip. Rev. Clim. Change* **2011**, *2*, 45–65. [CrossRef]
12. Centre for Emergency Situations and Disaster Risk Reduction. *Issledovanie po Otsenke Problem Zasukhi i Modelei Monitoringa Zasukh v Tsentral'noi Azii*; Salnikov, V.G., Ed.; Centre for Emergency Situations and Disaster Risk Reduction: Astana, Kazakhstan, 2020; 57p.
13. Brunner, M.I.; Götte, J.; Schlemper, C.; Van Loon, A.F. Hydrological drought generation processes and severity are changing in the Alps. *Geophys. Res. Lett.* **2023**, *50*, e2022GL101776. [CrossRef]
14. Trenberth, K.E.; Dai, A.; Van der Schrier, G.; Jones, P.D.; Barichivich, J.; Briffa, K.R.; Sheffield, J. Global warming and changes in drought. *Nat. Clim. Change* **2014**, *4*, 17–22. [CrossRef]
15. Mukherjee, S.; Mishra, A.; Trenberth, K.E. Climate change and drought: A perspective on drought indices. *Curr. Clim. Change Rep.* **2018**, *4*, 145–163. [CrossRef]
16. Ault, T.R. On the essentials of drought in a changing climate. *Science* **2020**, *368*, 256–260. [CrossRef] [PubMed]
17. Guo, H.; Bao, A.; Liu, T.; Jiapaer, G.; Ndayisaba, F.; Jiang, L.; Kurban, A.; De Maeyer, P. Spatial and temporal characteristics of droughts in Central Asia during 1966–2015. *Sci. Total Environ.* **2018**, *624*, 1523–1538. [CrossRef] [PubMed]
18. Chen, F.; Dong, G.; Chen, J.; Gao, Y.; Huang, W.; Wang, T.; Chen, S.; Hou, J. Climate change and silk road civilization evolution in arid Central Asia: Progress and issues. *Adv. Earth Sci.* **2019**, *34*, 561–572.
19. *SP 33-101-2003*; Determination of the Main Design Hydrological Characteristics. Gosstroy of Russia: Moscow, Russia, 2004.
20. Alexandersson, H. A homogeneity test applied to precipitation data. *J. Climatol.* **1986**, *6*, 661–675. [CrossRef]
21. Alexandersson, H.; Moberg, A. Homogenization of Swedish temperature data. Part I: Homogeneity test for linear trends. *Int. J. Climatol.* **1997**, *17*, 25–34. [CrossRef]
22. Khalil, A. Inhomogeneity detection in the rainfall series for the Mae Klong River Basin, Thailand. *Appl. Water Sci.* **2021**, *11*, 147. [CrossRef]
23. Pettitt, A.N. A non-parametric approach to the change-point problem. *Appl. Stat.* **1979**, *28*, 126–135. [CrossRef] [PubMed]
24. Buishand, T.A. Some methods for testing the homogeneity of rainfall records. *J. Hydrol.* **1982**, *58*, 11–27. [CrossRef]
25. Page, E.S. Continuous inspection schemes. *Biometrika* **1954**, *41*, 100–115. [CrossRef]

26. McKee, T.B.; Doesken, N.J.; Kleist, J. The relationship of drought frequency and duration to time scales. In Proceedings of the 8th Conference on Applied Climatology, Anaheim, CA, USA, 17–22 January 1993; pp. 179–184.
27. Allen, R.G.; Pereira, L.S.; Raes, D.; Smith, M. *Crop Evapotranspiration—Guidelines for Computing Crop Water Requirements*; FAO: Rome, Italy, 1998. Available online: https://www.researchgate.net/publication/235704197_Crop_evapotranspiration-Guidelines_for_computing_crop_water_requirements-FAO_Irrigation_and_drainage_paper_56 (accessed on 1 September 2026).
28. Vicente-Serrano, S.M.; Beguería, S.; López-Moreno, J.I. A multiscalar drought index sensitive to global warming: The standardized precipitation evapotranspiration index. *J. Clim.* **2010**, *23*, 1696–1718. [CrossRef]
29. Nalbantis, I.; Tsakiris, G. Assessment of hydrological drought revisited. *Water Resour. Manag.* **2009**, *23*, 881–897. [CrossRef]
30. Spearman, C. The proof and measurement of association between two things. *Am. J. Psychol.* **1904**, *15*, 72–101. [CrossRef] [PubMed]
31. Sun, X.J.; Wang, P.X.; Wang, J.X.L. An assessment of the atmospheric centers of action in the northern hemisphere winter. *Clim. Dyn.* **2017**, *48*, 1031–1047. [CrossRef]
32. Dai, A. Increasing drought under global warming in observations and models. *Nat. Clim. Change* **2013**, *3*, 52–58. [CrossRef]
33. Sun, Y.; Chen, X.; Yu, Y.; Qian, J.; Wang, M.; Huang, S.; Xing, X.; Song, S.; Sun, X. Spatiotemporal characteristics of drought in Central Asia from 1981 to 2020. *Atmosphere* **2022**, *13*, 1496. [CrossRef]
34. Mwinjuma, M.; Wang, R.; Mtupili, M.; Twaha, M. Comparisons of SPI and SPEI in capturing drought dynamics: A global assessment across arid and humid regions. *Atmos. Res.* **2026**, *329*, 108475. [CrossRef]
35. Cook, B.I.; Mankin, J.S.; Anchukaitis, K.J. Climate change and drought: From past to future. *Curr. Clim. Change Rep.* **2018**, *4*, 164–179. [CrossRef]
36. Worku, M.A. Spatiotemporal analysis of drought severity using SPI and SPEI: Case study of semi-arid Borana area, southern Ethiopia. *Front. Environ. Sci.* **2024**, *12*, 1337190. [CrossRef]
37. Cui, A.; Li, J.; Zhou, Q.; Zhu, H.; Liu, H.; Yang, C.; Wu, G.; Li, Q. Propagation dynamics from meteorological drought to GRACE-based hydrological drought and its influencing factors. *Remote Sens.* **2024**, *16*, 976. [CrossRef]
38. Samim, A.T.; Lee, H.S.; Hussainzada, W.; Bhanage, V.; Nayyer, F. Comprehensive drought assessment based on the SPEI and its impact on crop production and streamflow in Afghanistan. *J. Hydrol. Reg. Stud.* **2025**, *62*, 102893. [CrossRef]
39. Van Loon, A.F. Hydrological drought explained. *Water* **2015**, *2*, 359–392. [CrossRef]
40. Long, Y.; Huang, Y.; Ma, Q.; Yu, W.; Tan, C. Future drought patterns in Southwest China: A CMIP6-based analysis using multiple drought indices. *J. Hydrol. Reg. Stud.* **2025**, *61*, 102702. [CrossRef]

Disclaimer/Publisher's Note: The statements, opinions and data contained in all publications are solely those of the individual author(s) and contributor(s) and not of MDPI and/or the editor(s). MDPI and/or the editor(s) disclaim responsibility for any injury to people or property resulting from any ideas, methods, instructions or products referred to in the content.